in parental UCSD/AML1 cells and AML1/Nega cells at 24 h after stimulation. These results suggest that Ang1 expression negatively regulates cell cycle progression from G0/G1 to S phase in UCSD/AML1 cells.

Because Ang1 is known to be an important factor in the maintenance of the quiescent state of HSCs in the bone marrow niche, we next investigated whether Ang1 is associated with the maintenance of G0 phase in EVI1^{high} leukemia cells. We measured the percentages of G0 phase of cell population by double staining with Ki67 and 7-AAD at just before and 18 h after serum stimulation of starved AML1/shAng1, AML1/shNega or parental cells. At just before stimulation, the percentages of cells in G0 phase were not significantly different between AML1/shAng1 and control cells, but they were significantly lower in AML1/shAng1-1 and -2 cells (14–16%) than in parental UCSD/AML1 cells or AML1/Nega cells (20–22%) at 18 h after stimulation (Fig. 3D and Supplementary Fig. 1). These results show that knockdown of Ang1 expression did not influence entry into G0 phase during serum starvation, but it enhanced exit from G0 phase after serum stimulation, suggesting that Ang1 may inhibit cell cycle re-entry from the quiescent state.

3.4. Ang1 regulates p18 gene expression through Ang1/Tie2 signaling in EVI1^{high} leukemia cells

To clarify how Ang1 regulates the cell cycle in UCSD/AML1 cells, we assessed the gene expression levels of cyclin-dependent kinases (CDK4 and CDK6), CDK inhibitors (p21, p27, p18, and p57), and cell adhesion molecules (β1 integrin and β2 integrin) by semi-quantitative RT-PCR. Compared with parental UCSD/AML1 cells or AML1/shNega cells, p18 mRNA was clearly decreased in AML1/shAng1-1 and -2 cells (Fig. 4A), and the downregulation of p18 in AML1/shAng1-1 and -2 cells was also confirmed using quantitative RT-PCR (Fig. 4B). In addition, the expression of p18 was down-regulated in primary AML cells introduced with shAng1 (PT11/shAng1) (Fig. 4C and D). We next determined how Ang1 expression regulates the expression of p18 in EVI1^{high} leukemia cells. Because Ang1 is a secreted Tie2 ligand, we hypothesized that the Ang1 protein secreted from an EVI1^{high} leukemia cell would bind to Tie2 receptors, thereby activating a signaling pathway leading to p18 expression in the nucleus. To confirm whether the secreted Ang1 binds to Tie2 and regulates the expression of p18, recombinant human Tie2/Fc chimeric protein, which acts as a decoy receptor, was added to the medium of UCSD/AML1 and PT11 cells, and the expression levels of p18 were monitored. Quantitative RT-PCR analysis showed that p18 expression levels were decreased in the cells treated with Tie2/Fc (Fig. 4E and F). We then examined p18 gene expression levels in five leukemia cell samples from EVI1^{high} AML patients and eight leukemia cell samples from EVI1^{low} AML patients using quantitative RT-PCR. Significant correlations were found between the expression of Ang1 and p18 (Fig. 4G). Taken together, these results suggest that secreted Ang1 up-regulates p18 gene expression through Ang1/Tie2 signaling, resulting in a delay in cell cycle progression in EVI1^{high} leukemia cells.

4. Discussion

In this study, we demonstrated that Ang1 is highly expressed in EVI1^{high} leukemia cells in a manner dependent on EVI1 expression. Moreover, we showed that in EVI1^{high} leukemia cells, Ang1 suppresses cell cycle progression via maintenance of G0/G1 phase and up-regulates the expression of p18 through Ang1/Tie2 signaling. Because EVI1^{high} AML entails a poor prognosis and is resistance to chemotherapy, our results suggest that the expression of the negative cell cycle regulator p18 in response to active Ang1/Tie2 signaling may maintain EVI1^{high} leukemia cells in G0/G1 phase, which may help to maintain them in the bone marrow niche, resulting in resistance to chemotherapy.

It has been reported that treatment of HSCs with Ang1 up-regulates the expression of the CDK inhibitors p18 and p57 along with that of Itgb1 and Tie2 [29], whereas expression of p57, Itgb1, and Tie2 is not influenced by knocking down Ang1 expression in UCSD/AML1 and PT11 cells, suggesting that p18 may be an important downstream factor regulating the cell cycle in response to Ang1/Tie2 signaling in EVI1^{high} leukemia cells. Moreover, p18 has been hypothesized to preserve HSC function by limiting their cell-cycle entry [30], and Nurr1, a nuclear receptor transcription factor, maintains the quiescence of HSCs through up-regulation of p18 gene expression [31]. Therefore, p18 may also play an important role in maintaining the stem cell-like phenotypes of EVI1^{high} leukemia cells. Ang1/Tie2 signaling between quiescent HSCs and the endosteal niche contributes to the maintenance of HSCs and protects them against various cellular stresses [17]. Because the resistance of leukemia cells to anti-cancer drugs is known to be dependent on cell quiescence in the bone marrow niche, the maintenance of stem cell-like phenotypes by p18 through the activation of Ang1/Tie2 signaling may be related to leukemia cell chemoresistance and thereby contribute to a poor prognosis.

It was reported that AML patients expressing high levels of Ang2 had significantly longer overall survival after chemotherapy than those with low Ang2 levels [32]. Because Ang2 is a Tie2 receptor antagonist, inactivation of Ang1/Tie2 signaling may lead to a favorable prognosis. This is consistent with our view that the maintenance of cell quiescence by active Ang1/Tie2 signaling is probably a main reason for the poor prognosis of EVI1^{high} AML patients. Therefore, inhibiting Ang1/Tie2 signaling may enhance sensitivity to chemotherapy by inducing cell cycle entry from quiescence, and combining an inhibitor of Ang1/Tie2 signaling with other anti-cancer drugs may be an effective treatment for EVI1^{high} AML. We hope that inhibitors of the Ang1/Tie2 signaling will be applied to clinical trials, which may contribute to improved patient outcomes.

Acknowledgment

This work was supported by Grants-in-Aid for Scientific Research in Priority Areas from the Ministry of Education, Culture, Sports, Science and Technology in Japan.

Appendix A. Supplementary data

Supplementary data associated with this article can be found, in the online version, at doi:10.1016/j.bbrc.2011.10.061.

References

[1] K. Morishita, D.S. Parker, M.L. Mucenski, et al., Retroviral activation of a novel gene encoding a zinc finger protein in IL-3-dependent myeloid leukemia cell lines, Cell 54 (1988) 831–840.
[2] M.L. Mucenski, B.A. Taylor, J.N. Ihle, et al., Identification of a common ecotropic viral integration site, EVI-1, in the DNA of AKXD murine myeloid tumors, Mol. Cell. Biol. 8 (1988) 301–308.
[3] K. Morishita, E. Parganas, C.L. William, et al., Activation of EVI1 gene expression in human acute myelogenous leukemias by translocations spanning 300–400 kilobases on chromosome band 3q26, Proc. Natl Acad. Sci. USA 89 (1992) 3937–3941.
[4] K. Mitani, S. Ogawa, T. Tanaka, et al., Generation of the AML1–EVI-1 fusion gene in the t(3;21)(q26;q22) causes blastic crisis in chronic myelocytic leukemia, EMBO J. 13 (1994) 504–510.
[5] S. Lugthart, E. van Drunen, Y. van Norden, et al., High EVI1 levels predict adverse outcome in acute myeloid leukemia: prevalence of EVI1 overexpression and chromosome 3q26 abnormalities underestimated, Blood 111 (2008) 4329–4337.

[6] P.J. Valk, R.G. Verhaak, M.A. Beijen, et al., Prognostically useful gene-expression profiles in acute myeloid leukemia, N. Engl. J. Med. 350 (2004) 1617–1628.
[7] S. Barjesteh van Waalwijk van Doorn-Khosrovani, C. Erpelinck, W.L. van Putten, et al., High EVI1 expression predicts poor survival in acute myeloid leukemia: a study of 319 de novo AML patients, Blood 101 (2003) 837–845.
[8] R.L. Phillips, R.E. Ernst, B. Brunk, et al., The genetic program of hematopoietic stem cells, Science 288 (2000) 1635–1640.
[9] I.K. Park, Y. He, F. Lin, et al., Differential gene expression profiling of adult murine hematopoietic stem cells, Blood 99 (2002) 488–498.
[10] S. Shimizu, T. Nagasawa, O. Katoh, et al., EVI1 is expressed in megakaryocyte cell lineage and enforced expression of EVI1 in UT-7/GM cells induces megakaryocyte differentiation, Biochem. Biophys. Res. Commun. 292 (2002) 609–616.
[11] H. Yuasa, Y. Oike, A. Iwama, et al., Oncogenic transcription factor evi1 regulates hematopoietic stem cell proliferation through GATA-2 expression, EMBO J. 24 (2005) 1976–1987.
[12] S. Goyama, G. Yamamoto, M. Shimabe, et al., EVI-1 is a critical regulator for hematopoietic stem cells and transformed leukemic cells, Cell Stem Cell 3 (2008) 207–220.
[13] S. Davis, T.H. Aldrich, P.F. Jones, et al., Isolation of angiopoietin-1, a ligand for the TIE2 receptor, by secretion-trap expression cloning, Cell 87 (1996) 1161–1169.
[14] C. Suri, P.F. Jones, S. Patan, et al., Requisite role of angiopoietin-1, a ligand for the TIE2 receptor, during embryonic angiogenesis, Cell 87 (1996) 1171–1180.
[15] P.C. Maisonpierre, C. Suri, P.F. Jones, et al., Angiopoietin-2, a natural antagonist for Tie2 that disrupts in vivo angiogenesis, Science 277 (1997) 55–60.
[16] D.M. Valenzuela, J.A. Griffiths, J. Rojas, et al., Angiopoietins 3 and 4: diverging gene counterparts in mice and humans, Proc. Natl Acad. Sci. USA 96 (1999) 1904–1909.
[17] F. Arai, A. Hirao, M. Ohmura, et al., Tie2/angiopoietin-1 signaling regulates hematopoietic stem cell quiescence in the bone marrow niche, Cell 118 (2004) 149–161.
[18] K.A. Moore, I.R. Lemischka, "Tie-ing" down the hematopoietic niche, Cell 118 (2004) 139–140.
[19] J. Oval, O.W. Jones, M. Montoya, et al., Characterization of a factor-dependent acute leukemia cell line with translocation (3;3)(q21;q26), Blood 76 (1990) 1369–1374.
[20] J. Oval, M. Smedsrud, R. Taetle, Expression and regulation of the EVI-1 gene in the human factor-dependent leukemia cell line, UCSD/AML1, Leukemia 6 (1992) 446–451.
[21] H. Hamaguchi, K. Suzukawa, K. Nagata, et al., Establishment of a novel human myeloid leukaemia cell line (HNT-34) with t(3;3)(q21;q26), t(9;22)(q34;q11) and the expression of EVI1 gene, P210 and P190 BCR/ABL chimaeric transcripts from a patient with AML after MDS with 3q21q26 syndrome, Br. J. Haematol. 98 (1997) 399–407.
[22] H. Asou, K. Suzukawa, K. Kita, et al., Establishment of an undifferentiated leukemia cell line (Kasumi-3) with t(3;7)(q27;q22) and activation of the EVI1 gene, Jpn. J. Cancer Res. 87 (1996) 269–274.
[23] P. Martin, T. Papayannopoulou, HEL cells: a new human erythroleukemia cell line with spontaneous and induced globin expression, Science 216 (1982) 1233–1235.
[24] R. Gallagher, S. Collins, J. Trujillo, et al., Characterization of the continuous, differentiating myeloid cell line (HL-60) from a patient with acute promyelocytic leukemia, Blood 54 (1979) 713–733.
[25] C. Sundstrom, K. Nilsson, Establishment and characterization of a human histiocytic lymphoma cell line (U-937), Int. J. Cancer 17 (1976) 565–577.
[26] C.B. Lozzio, B.B. Lozzio, Human chronic myelogenous leukemia cell-line with positive Philadelphia chromosome, Blood 45 (1975) 321–334.
[27] Y. Matsuo, T. Adachi, T. Tsubota, et al., Establishment and characterization of a novel megakaryoblastic cell line, MOLM-1, from a patient with chronic myelogenous leukemia, Hum. Cell 4 (1991) 261–264.
[28] Y. Saito, S. Nakahata, N. Yamakawa, et al., CD52 as a molecular target for immunotherapy to treat acute myeloid leukemia with high EVI1 expression, Leukemia 25 (2011) 921–931.
[29] Y. Gomei, Y. Nakamura, H. Yoshihara, et al., Functional differences between two Tie2 ligands, angiopoietin-1 and -2, in regulation of adult bone marrow hematopoietic stem cells, Exp. Hematol. 38 (2010) 82–89.
[30] H. Yu, Y. Yuan, H. Shen, et al., Hematopoietic stem cell exhaustion impacted by p18 INK4C and p21 Cip1/Waf1 in opposite manners, Blood 107 (2006) 1200–1206.
[31] O. Sirin, G.L. Lukov, R. Mao, et al., The orphan nuclear receptor Nurr1 restricts the proliferation of haematopoietic stem cells, Nat. Cell Biol. 12 (2010) 1213–1219.
[32] C. Schliemann, R. Bieker, T. Padro, et al., Expression of angiopoietins and their receptor Tie2 in the bone marrow of patients with acute myeloid leukemia, Haematologica 91 (2006) 1203–1211.

Oncogene (2011) 30, 4194–4207

www.nature.com/onc

ORIGINAL ARTICLE

Sumoylation of MEL1S at lysine 568 and its interaction with CtBP facilitates its repressor activity and the blockade of G-CSF-induced myeloid differentiation

I Nishikata, S Nakahata, Y Saito, K Kaneda, E Ichihara, N Yamakawa and K Morishita

Division of Tumor and Cellular Biochemistry, Department of Medical Sciences, Faculty of Medicine, University of Miyazaki, Miyazaki, Japan

MEL1 **(MDS1/EVI1-like gene 1/*PRDM16*), which was identified as a gene near the chromosomal breakpoint in t(1;3)(p36;q21)-positive human acute myeloid leukemia cells, belongs to the PRDI-BF1-RIZ1 homologous (PR) domain (PRDM) family of transcription repressors. The short form of MEL1 (MEL1S), which lacks the PR-domain at the *N*-terminus, is the main form expressed in t(1;3)(p36;q21)-positive acute myeloid leukemia cells. The overexpression of MEL1S blocks granulocyte colony-stimulating factor (G-CSF)-induced myeloid differentiation in interleukin-3-dependent murine myeloid L-G3 cells. In this study, we show that treatment with the histone deacetylase inhibitor trichostatin A abolished the blockade of myeloid differentiation in L-G3 cells overexpressing MEL1S. The expression of MEL1S containing mutated CtBP-interacting motif (CIM) in L-G3 cells still blocked the myeloid differentiation induced by G-CSF. We found that the small ubiquitin-related modifier (SUMO) motif (SM) at lysine 568 (VKAE) adjacent to the CIM was necessary to obtain the maximum transcriptional repressor activity of MEL1S. L-G3 cells expressing MEL1S, and bearing mutated CIM and SM differentiated into granulocytes in response to G-CSF; this indicated that both the SUMO modification at lysine 568 and CtBP binding were required for MEL1S-mediated transcriptional repression and blockade of differentiation, which might be relevant for the process of leukemogenesis.**
Oncogene (2011) **30,** 4194–4207; doi:10.1038/onc.2011.132; published online 25 April 2011

Keywords: MEL1; sumoylation; CtBP; G-CSF

Introduction

Acute myeloid leukemia with reciprocal translocation t(1;3)(p36;q21) is frequently characterized by trilineage dysplasia, particularly dysmegakaryocytopoiesis, and a poor prognosis (Moir *et al.*, 1984; Bloomfield *et al.*, 1985; Welborn *et al.*, 1987). These clinical features are very similar to those of the 3q21q26 syndrome, which is characterized by a high expression of the ecotropic viral integration site-1 (*EVI1*) gene (Shimizu *et al.*, 2000). EVI1 (also called PR domain member 3 or PRDM3) is a zinc-finger transcription factor and belongs to the PRDI-BF1-RIZ1 homologous (PR) domain family (Morishita, 2007). We previously identified the MDS1/EVI1-like gene 1 (*MEL1*) as a member of the *EVI1* gene family and also as a PR domain family member (*PRDM16*); this gene is located near the chromosomal breakpoint at chromosome 1p36 of t(1;3)(p36;q21) (Mochizuki *et al.*, 2000; Shimizu *et al.*, 2000). PR-domain deficient forms of EVI1 and MEL1 (MEL1S) are upregulated in both types of leukemia (Mochizuki *et al.*, 2000; Nishikata *et al.*, 2003). We discovered that the overexpression of MEL1S in murine interleukin-3 (IL-3)-dependent myeloid L-G3 cells blocked the granulocytic differentiation induced by granulocyte colony-stimulating factor (G-CSF) (Nishikata *et al.*, 2003). Using the GAL4 DNA-binding domain (DBD) fused to MEL1 and MEL1S, we also identified that both MEL1 and MEL1S function as transcriptional repressors (Nishikata *et al.*, 2003).

EVI1 and MEL1 also belong to a family of transcription factors with *C*-terminal-binding protein (CtBP)-interacting motif (CIM) (Shimahara *et al.*, 2010). EVI1 has two CIMs, PFDLT (aa 553–559) and PLDLS (aa 584–590), and the repressor and cell-transforming functions of EVI1 are mediated by its CtBP-binding activity (Izutsu *et al.*, 2001). Moreover, MEL1/PRDM16 also has two CIMs, PFDLT (aa588–592) and PLDLS (aa 616–620), and was reported to directly interact with a CtBP co-repressor complex on the promoter of white fat-specific genes (Kajimura *et al.*, 2008).

CtBP was originally identified as a transcriptional co-repressor of the adenoviral E1A protein (Schaeper *et al.*, 1995). In addition, among transcription factors containing zinc-finger repeats, BKLF, ZEB1, ZEB2 (Shimahara *et al.*, 2010) and ZNF217 (Quinlan *et al.*, 2006) have been reported to have CIM. The CtBP co-repressor complex contains a number of epigenetic regulatory factors that mediate coordinated histone modification by deacetylation and methylation of histone H3

Correspondence: Dr K Morishita, Division of Tumor and Cellular Biochemistry, Department of Medical Sciences, Faculty of Medicine, University of Miyazaki, 5200 Kihara, Kiyotake, Miyazaki 889-1692, Japan.
E-mail: kmorishi@med.miyazaki-u.ac.jp
Received 25 November 2010; revised and accepted 19 March 2011; published online 25 April 2011

at lysine 9 and demethylation of histone H3 at lysine 4 (Chinnadurai, 2007). CtBP also recruits the small ubiquitin-related modifier (SUMO) and conjugates the E2 enzyme UBC9 and a SUMO E3 ligase (HPC2) (Kagey *et al.*, 2003). Therefore, it is possible that sumoylation might also be involved in CtBP-mediated transcriptional regulation.

In this study, we investigated whether the transcriptional repressor activity of MEL1 could mediate the blockade of the granulocytic differentiation of L-G3 cells induced by G-CSF. The L-G3 cells treated with the histone deacetylase (HDAC) inhibitor trichostatin A (TSA) overcame blockade of the G-CSF-induced differentiation by MEL1S expression. Here, the transcriptional repression by MEL1S is reported to be mediated by sumoylation and its interaction with CtBP. MEL1S interacted with the E2-conjugating enzyme UBC9, which led to sumoylation, and interacted with the transcriptional co-repressor CtBP. Site-directed mutagenesis and deletion analysis identified lysine 568 as a sumoylation site in MEL1S. Mutations of both the sumoylation site and the CIMs in MEL1S completely abrogated the repressor activity and released the MEL1S-induced differentiation block in L-G3 cells. Therefore, the transcriptional repressor activity of MEL1S is likely one of the important determinants in the development of leukemia.

Results

Combining G-CSF with TSA treatment overcomes the blockade of G-CSF-induced differentiation in murine L-G3 cells induced by MEL1S expression

We previously reported that the short form of MEL1 (MEL1S), a transcription factor that is specifically expressed in acute myeloid leukemia with the t(1;3) translocation, could block G-CSF-induced myeloid differentiation of L-G3, an IL-3-dependent myeloid leukemia cell line (Nishikata *et al.*, 2003). Because MEL1S works as a transcriptional repressor in hematopoietic cells, including L-G3 cells (Supplementary Figure 1), we initially investigated whether treatment of L-G3 cells with the HDAC inhibitor TSA prevents the blockade of G-CSF-induced differentiation by MEL1S expression. A series of L-G3 cell lines, consisting of parental cells or cells transfected with a Mock-vector (L-G3/Mock) or a MEL1S expression vector (L-G3/MEL1S), were cultured with IL-3, G-CSF or G-CSF with TSA for 6 days, and their cell growth, morphology and expression of myeloperoxidase (*Mpo*) and lactoferrin (*Lf*) (Friedman *et al.*, 1991), both of which are markers of granulocyte differentiation, were determined. At 6 days after treatment with G-CSF, most of the parental L-G3 cells and L-G3/Mock cells exhibited reduced cell growth, increased cell death, differentiation to granulocytes with multi-lobulated nuclei and expression of *Mpo* and *Lf*; however, the majority of L-G3/MEL1S cells grew well and remained undifferentiated myeloid cells with no *Mpo* and *Lf* expression (Figures 1a–d). At 6 days after treatment with G-CSF and TSA, the majority of the L-G3/MEL1S cells stopped growing and lost viability; the surviving cells differentiated into granulocytes and expressed *Mpo* and *Lf*. The L-G3/MEL1S cells treated with G-CSF and TSA survived 1–2 days longer than the G-CSF-treated control L-G3 cells, even though the surviving cells differentiated into mature granulocytes (Figures 1a and c). Therefore, TSA treatment, when combined with G-CSF, could release the blockade of granulocyte differentiation induced by MEL1S expression.

MEL1S lacking CtBP-interacting domain lost the transcriptional repressor activity

To determine the domain(s) of MEL1 that are responsible for transcriptional repression, we constructed a series of deletion mutants of MEL1S fused with the DBD of GAL4 (GAL4-DBD/MEL1) driven by the SV40 promoter. These mutants represent deletions of zinc-finger repeats 1–7 in the DBD1 (ΔDBD1), the proline-rich region (ΔPRR), the CtBP-interacting domain (CID) (ΔCID), the repressor domain (ΔRD), zinc-finger repeats 8–10 in the DBD2 (ΔDBD2) and the *C*-terminal acidic amino-acid cluster region (ΔCT) (Figure 2a). Either wild-type (WT) GAL4-DBD/MEL1S or a deletion mutant plasmid was transfected along with the pG5proLuc reporter plasmid into COS-7 cells, and the protein expression of each construct was confirmed by immunoblot analysis (Figure 2b). At 2 days after transfection, repression activity was measured by comparing the luciferase enzyme activities for each deletion construct to WT MEL1S as a reference. The repression was clearly reduced with MEL1S/ΔDBD1, MEL1S/ΔCID or MEL1S/ΔRD; MEL1S/ΔCID showed almost no repressor activity compared with WT MEL1S. Therefore, the CID may be the most important domain for the repressor activity of MEL1S.

Amino-acid substitutions in the MEL1S CIMs block G-CSF-induced myeloid differentiation

To evaluate whether the repressor activity of the CID of MEL1S is dependent on binding to the CtBP co-repressor, a MEL1S mutant carrying four amino-acid substitutions in the two CIMs (Shimahara *et al.*, 2010), which are located at amino-acids 588–592 (PFDLT) and 618–622 (PLDLS) (Figure 3a), was constructed. The aspartic acid and leucine at positions 560 and 561 in the first CIM (PFDLT) were replaced by alanine and serine (PFAST), and the aspartic acid and leucine at positions 660 and 661 in the second CIM (PLDLS) were replaced by alanine and serine (PLASS) to yield the CIM mutant (CIMmt) in the GAL4-DBD/MEL1 construct. To confirm the lack of CtBP-binding ability of the MEL1/CIMmt mutant, we transfected HA-tagged MEL1/WT, MEL1S/WT or MEL1S/CIMmt expression vectors with or without the FLAG-tagged CtBP2 expression vector into 293T cells. After immunoprecipitation using an anti-FLAG antibody, the precipitated proteins were detected using an anti-HA antibody, and CtBP2 was confirmed to bind MEL1 or MEL1S but not MEL1S/CIMmt (Figure 3b).

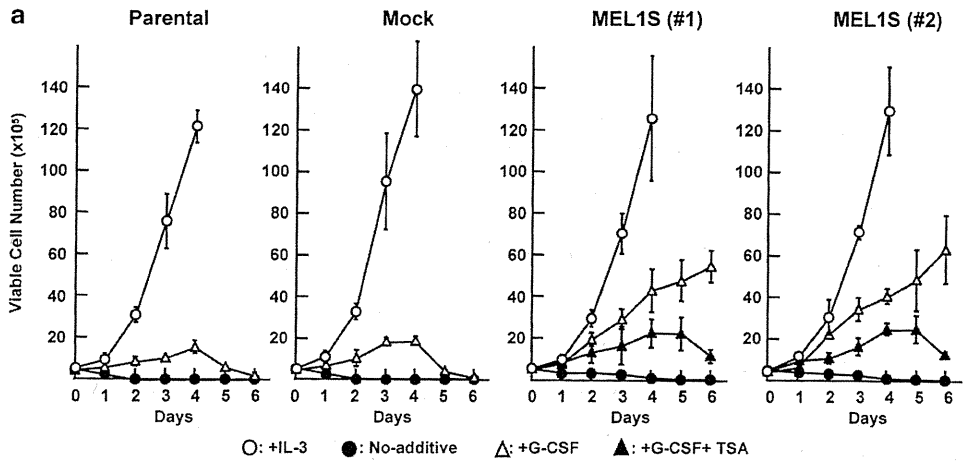
a
Parental
Mock
MEL1S (#1)
MEL1S (#2)
Viable Cell Number (x10³)
Days
O: +IL-3
●: No-additive
△: +G-CSF
▲: +G-CSF+ TSA

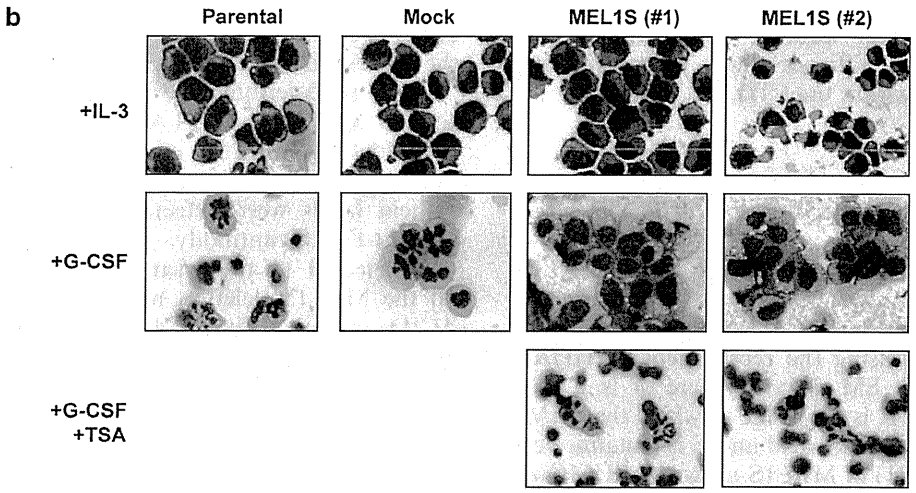
b
Parental
Mock
MEL1S (#1)
MEL1S (#2)
+IL-3
+G-CSF
+G-CSF
+TSA

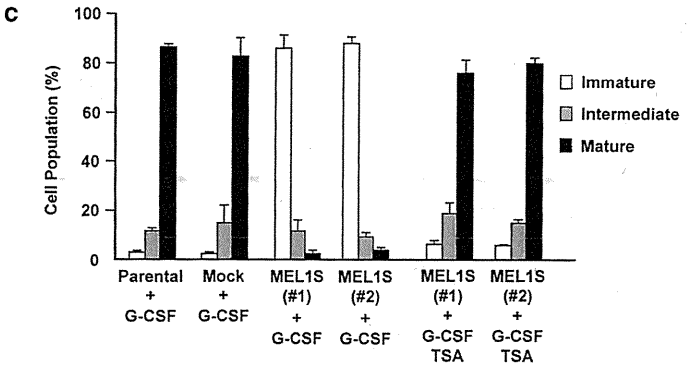
c
Cell Population (%)
Immature
Intermediate
Mature
Parental + G-CSF
Mock + G-CSF
MEL1S (#1) + G-CSF
MEL1S (#2) + G-CSF
MEL1S (#1) + G-CSF TSA
MEL1S (#2) + G-CSF TSA

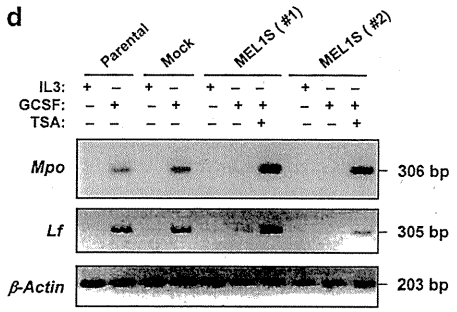
d
Parental
Mock
MEL1S (#1)
MEL1S (#2)
IL3:
GCSF:
TSA:
Mpo
Lf
β-Actin
306 bp
305 bp
203 bp

Next, a study was conducted on whether the expression of MEL1S/CIMmt could block G-CSF-induced myeloid differentiation of the L-G3 cell line. After transfection of the FLAG-tagged MEL1S/CIMmt expression vector into L-G3 cells, two L-G3/CIMmt cell lines were selected by G418 treatment and established. After confirming the MEL1 expression by immunoblot analysis with an anti-FLAG antibody (Figure 3c), the L-G3/MEL1S/CIMmt, L-G3 parental, L-G3/Mock and L-G3/MEL1S cells were treated with IL-3 or G-CSF for 6 days and their growth, cell morphology and expression of *Mpo* and *Lf* were determined. Parental L-G3 and L-G3/Mock control cells differentiated into granulocytes characterized by increased *MPO* and *Lf* mRNA levels on treatment with G-CSF, but the L-G3/MEL1S and MEL1S/CIMmt cell lines did not differentiate and remained immature myeloid cells (Figures 3d–f). Therefore, there is probably another important element for the inhibition of differentiation, apart from the CtBP-binding sites, within the CID.

Adjacent to the CtBP-interacting consensus sequence, MEL1S is sumoylated at K568 in an UBC9-dependent manner

Several transfection factors with CIM, such as ZEB1, ZEB2 and BKLF, were reported to be modified by sumoylation, facilitating the transcriptional repressor function by increasing the recruitment of HDAC. We searched for the SM ψKxE (where ψ is a large hydrophobic residue, K is the lysine to which the SUMO is conjugated, x is any amino acid and E is glutamic acid) (Rodriguez *et al*., 2001) in MEL1S using the SUMOplot analysis program (ABGENT, http://www.abgent.com/tools/sumoplot). There are seven high-probability putative SUMO consensus sites (scores over 0.69) in MEL1S (Supplementary Table 1). Of these, lysine 568 (AHNLL VKAE PKSPR) and lysine 85 (GLAEE LKPE GLGGG) have the highest probability of sumoylation (scores over 0.9), and lysine 568 is located just 20 amino-acid residues upstream of the CIM (PFDLT), within the CID.

To test whether MEL1S could be covalently modified by sumoylation, the FLAG-MEL1S expression vector was transfected with GFP-fused SUMO1 (GFP/SUMO1) and the Myc-tagged conjugating enzyme UBC-9 (Myc/UBC9) or with GFP/SUMO1 and a dominant negative form of Myc/UBC-9 with cysteine 93 mutated to serine (Giorgino *et al*., 2000) into 293T cells. The cell lysates were subjected to sodium dodecyl sulfate (SDS)–PAGE and blotted with an anti-FLAG antibody. As shown in Figure 4a, a slowly migrating band of MEL1S was detected only in the lysates from cells transfected with SUMO1 and UBC9, but not in those expressing SUMO1 and UBC9 (C93S). To confirm whether the slowly migrating band of MEL1S corresponded to a sumoylated form of MEL1S, 293T cells were transfected under the same conditions as above, and the cell lysates were immunoprecipitated with an anti-FLAG antibody to bring down MEL1S. The precipitated proteins were then detected using an anti-FLAG or anti-GFP antibody. As shown in Figure 4b, the slower migrating band of MEL1S was detected by both antibodies, suggesting that this form of the protein likely represents a sumoylated MEL1S.

Next, to determine the location of the sumoylation site in MEL1S, six FLAG-tagged deletion mutants of MEL1S (illustrated in Figure 2a) were transfected into 293T cells along with SUMO1 and UBC9; MEL1S protein levels were detected by immunoblotting with an anti-FLAG antibody. A sumoylated MEL1S band was detected in the lysates of cells transfected with all the MEL1S deletion mutants, except the MEL1S/ΔCID mutant (Figure 4c). Therefore, the lysine(s) modified by sumoylation might be located within the CID. Because lysine 568 (AHNLL VKAE PKSPR), which lies within the CID, is one of the candidate lysines with a high sumoylation probability score (Supplementary Table 1), a MEL1S mutant was constructed with arginine substituted for lysine at position 568 (K568R; sumoylation motif mutant or SMmt) to determine whether MEL1S was sumoylated at lysine 568 (Figure 4d). After co-transfection with FLAG-tagged MEL1S, MEL1S/ΔCID, MEL1S/SMmt or MEL1S/CIMmt and SUMO1 and UBC9, MEL1S was detected by blotting with an anti-FLAG antibody. Sumoylated MEL1S was detected in the lysates of cells transfected with MEL1/WT or MEL1S/CIMmt but not with MEL1S/ΔCID or MEL1S/SMmt (Figure 4e), suggesting that lysine 568 is the sumoylated lysine within the CID.

Figure 1 TSA promotes G-CSF-dependent granulocytic differentiation in L-G3 cells overexpressing MEL1S. (**a**) Growth curves of L-G3 cells infected with a *MEL1S* retrovirus. IL-3-dependent murine myeloid L-G3 cells stably expressed either FLAG-tagged MEL1S (L-G3/MEL1S, #1 and #2, which correspond to lanes 3 and 4 in Figure 3c) or the mock vector (L-G3/Mock). The parental cells were grown under different culture conditions. Viable cells were counted using the trypan-blue exclusion method at each time point. Each culture condition was marked at the bottom of the figure. Open or closed circles indicate the culture conditions using medium with or without IL-3, respectively, and open or closed triangles indicate medium with G-CSF or G-CSF + TSA, respectively. The error bars represent the s.d. of three independent experiments. (**b**) May-Grünwald-Giemsa staining of cytospin preparations of parental and infected L-G3 cells after cultivation in IL-3 (top panel), G-CSF (middle panel) or G-CSF + TSA (bottom panel) for 6 days. Pictures were taken at × 100 magnification. (**c**) Comparison of cell populations estimated by counting stained nuclei after 6 days of culture in different media. The graph shows the results from two independent experiments; in each experiment, more than 100 cells were surveyed under the microscope. After culture in medium containing G-CSF alone or G-CSF with TSA, the cells were classified into the following three categories: immature, intermediate and mature. The population of cells in each category is expressed as the percentage (%) of the total cells. (**d**) Detection of myeloperoxidase *(Mpo)* and lactoferrin *(Lf)* expression in L-G3 transformants and parental cells cultured in medium containing IL-3, G-CSF or G-CSF + TSA for 6 days. Semi-quantitative RT–PCR was performed using specific primers for *Mpo* or *Lf*. RT–PCR for *β-Actin* was performed to test for equal loading. The sizes of the PCR products for *Mpo, Lf* and *β-Actin* are 306, 305 and 203 bp, respectively.

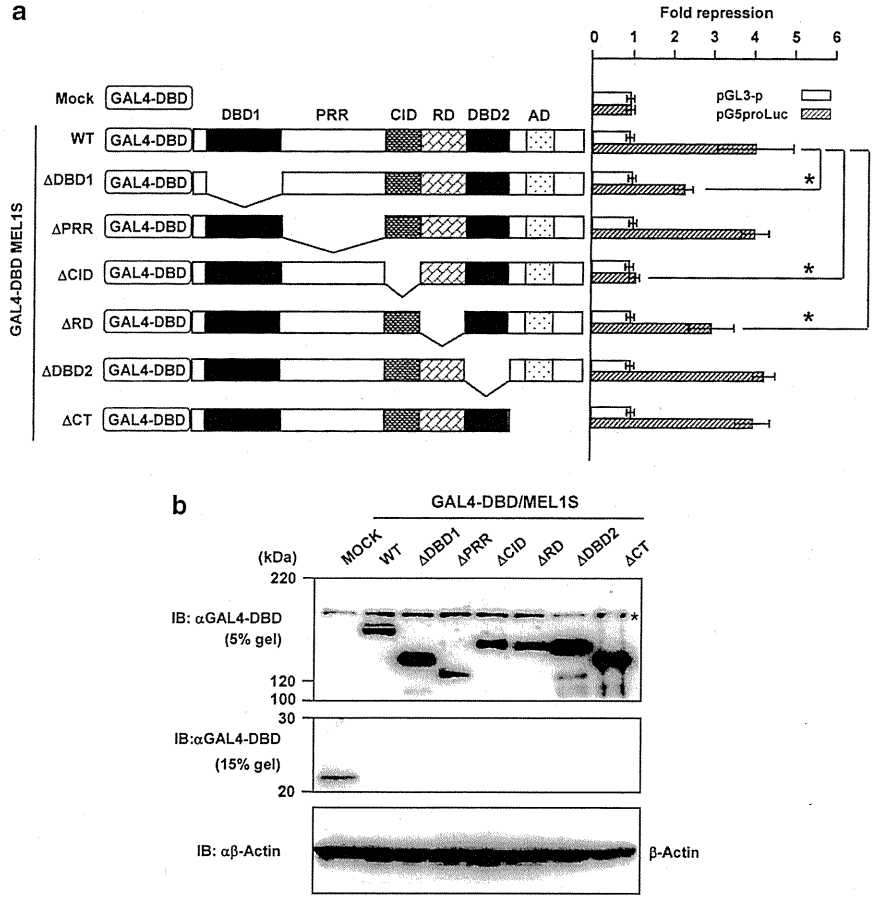

Figure 2 Transcriptional activities of MEL1S and the deletion mutants fused to the *C*-terminal end of the GAL4-DBD. (**a**) Repression activities of GAL4-DBD-fused MEL1S and its deletion mutants. COS-7 cells were co-transfected with the pGL3-promoter vector control (pGL3-p) or pG5proLuc with five consensus GAL4-binding sites (UAS) and the internal control plasmid pRL-MP together with the mock expression vector (GAL4-DBD), GAL4-DBD/MEL1S or the deletion mutants, as illustrated in Figure 2a. After 48 h of incubation, the cell extracts were prepared, and reporter activity was determined according to the manufacturer's instructions. Values of relative luciferase activity represent the mean ± s.d. of three independent transfections. $^*P<0.05$ (Student's *t*-test). (**b**) The protein expression levels of transfected MEL1S and the deletion mutants in COS-7 cells were determined by immunoblotting using the anti-GAL4-DBD antibody. The expression of GAL4–DBD/MEL1S fusion proteins (top panel) and Mock constructs (middle panel) were analyzed by 5 and 15% SDS–PAGE, respectively. β-Actin was used as an internal control. Molecular weight markers are given in kilodaltons (kDa). Stars indicate nonspecific bands.

Figure 3 Forced expression of the MEL1S mutant harboring disrupted CIM blocks G-CSF-induced granulocytic differentiation. (**a**) Schematic illustration of human MEL1S and the mutant form of MEL1S. PRD indicates the PR domain; DBD1, DNA-binding domain 1; PRR, the proline-rich region; CID, the CtBP-interacting domain; RD, the repression domain; DBD2, DNA-binding domain 2; and AD, the acidic domain. MEL1S has two CIMs (PFDLT and PLDLS). The motifs reside in the CID of MEL1S. The two CIMs, PFDLT and PLDLS, were mutated to PFAST and PLASS, respectively, by site-directed mutagenesis. (**b**) MEL1S interacts with CtBP2 through the CIM. HA-tagged MEL1, MEL1S or MEL1S/CIM mutant was transiently expressed with FLAG-tagged CtBP2 in 293T cells. HA-tagged MEL1 proteins and FLAG-CtBP2 were immunoprecipitated using an anti-HA antibody and an anti-FLAG antibody, respectively. The precipitated proteins were separated by SDS–PAGE and MEL1, MEL1S, the CIM mutant and/or CtBP2 were detected by western blotting (top panels). The inputs of each assay are shown on the bottom panels. (**c**) Expression of MEL1S (FLAG/MEL1S/WT) and the mutant (FLAG/MEL1S/CIMmt and FLAG/MEL1S/SMmt/CIMmt) clones in retrovirally infected L-G3 cell lines. Cell extracts from L-G3 cells infected with retrovirus containing FLAG-tagged MEL1S or its mutants were subjected to immunoblotting using the anti-FLAG antibody. Expression of β-Actin, which served as an internal control, is shown in the lower panel. Molecular weight markers are given in kDa. (**d**) Growth curves of L-G3 cells infected with retrovirus encoding a *MEL1S* mutant harboring disrupted CIM. L-G3 cells stably expressing either FLAG-tagged MEL1S (L-G3/MEL1S), the CtBP interaction mutant (L-G3/MEL1S/CIMmt, #1 and #2, which correspond to lanes 5 and 6 in Figure 3c), or the mock vector (L-G3/Mock) and the parental cells were grown under different culture conditions. Viable cells were counted by the trypan-blue exclusion method at each time point. Each culture condition is marked at the bottom of the figure. Open or closed circles indicate the culture conditions using medium with or without IL-3, respectively, and open triangles indicate medium with G-CSF. The error bars represent the s.d. of three independent experiments. (**e**) May-Grünwald-Giemsa staining of cytospin preparations of parental and infected L-G3 cells after cultivation in medium containing IL-3 (top panel) or G-CSF (bottom panel) for 6 days. Pictures were taken at × 100 magnification. (**f**) Detection of *Mpo* and *Lf* expression in L-G3 transformants and parental cells cultured in medium containing IL-3 or G-CSF for 6 days. Semi-quantitative RT–PCR was performed using *Mpo*- or *Lf*-specific primers.

Both sumoylation and CtBP binding in the CID are required for the transcriptional repressor function of MEL1S

To examine whether the transcriptional repressor activity of MEL1S is dependent on both sumoylation and CtBP binding in the CID, SM and CIMs, SM and CIMs double mutants (SM/CIMmt) were constructed in a GAL4 DBD-fused MEL1S expression vector (Figure 5a). After confirmation of the protein expression of each MEL1S expression plasmid by western blotting

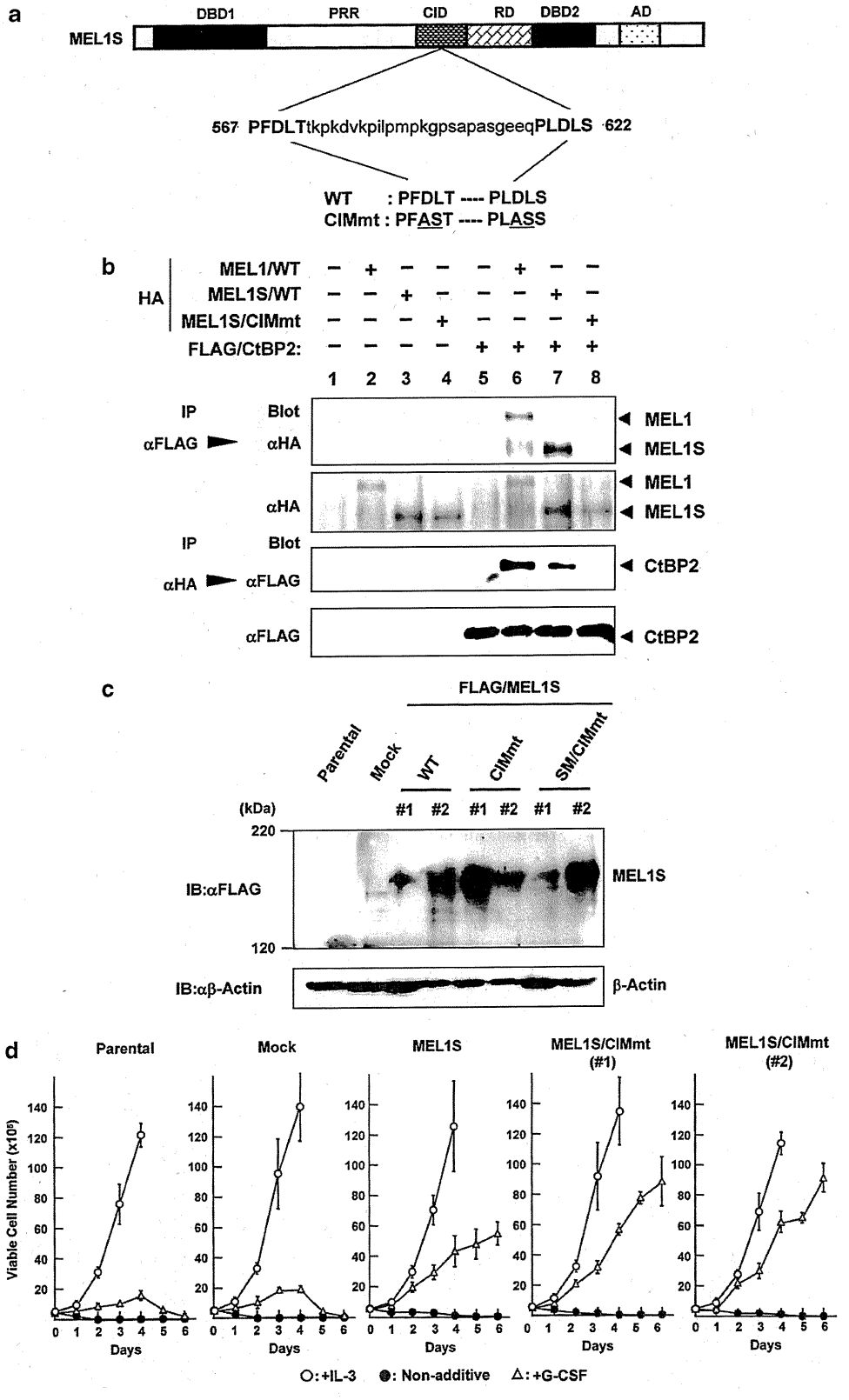

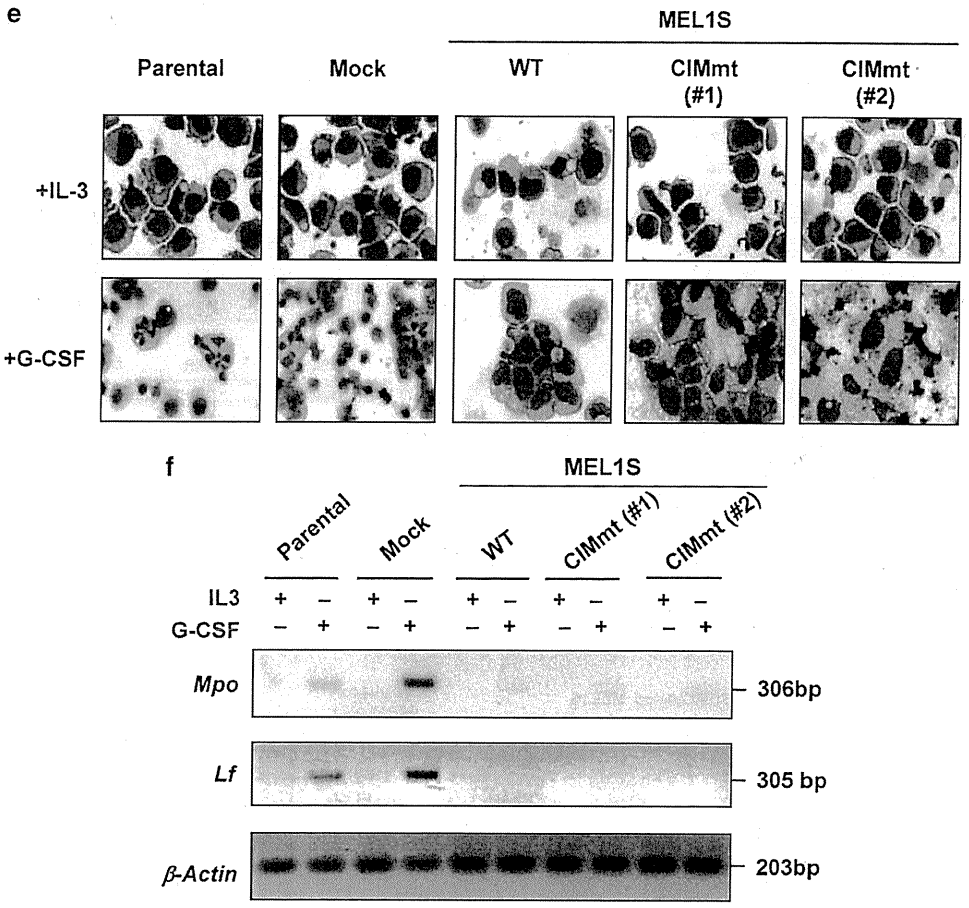

Figure 3 Continued.

(Figure 5b), each MEL1S construct (/WT,/ΔCID,/SMmt,/CIMmt, and SM/CIMmt) was analyzed for transcriptional repressor activity by co-transfection with the pG5proLuc reporter in COS-7 cells. MEL1S/WT-induced repression of the transcription by approximately fivefold, but MEL1S/ΔCID exhibited very little repressive activity (Figure 5a). The repressive activity of MEL1S/SMmt was slightly reduced compared with that of MEL1S/WT, and the activity of MEL1S/CIMmt was moderately reduced. Interestingly, the repression activity of MEL1S/SM/CIMmt was negligible, suggesting that both the sumoylation and the CtBP-binding property might contribute to the transcriptional repressor activity of MEL1S.

HDAC interacts with the sumoylated and CtBP-interacting regions in the CID of MEL1S

Because transcriptional repression by MEL1S may involve the recruitment of HDAC, the binding of HDAC to the SM and CIMs was assessed in the CID of MEL1S as EVI1 (Mitani, 2004; Maki *et al.*, 2008). For this experiment, the expression vectors were constructed containing a GFP-fused CID (GFP/CID) containing various mutations, such as CID/SMmt, CID/CIMmt or CID/SM/CIMmt (Figure 6a), which contain the same amino-acid substitutions as in Figures 3a and 4d. These constructs were transfected with or without a FLAG-tagged HDAC2 expression vector into 293T cells, and the cell lysates were immunoprecipitated with an anti-FLAG M2 affinity gel. The precipitated proteins were detected using an anti-GFP antibody. The precipitated GFP/CID protein was clearly detected in the lysates of cells transfected with GFP/CID/WT, but the level of the GFP/CID protein was clearly decreased with the GFP/CID/SMmt and GFP/CID/CIMmt expression vectors (Figure 6b). Moreover, the GFP/CID/SM/CIMmt protein was not co-immunoprecipitated with FLAG-HDAC2, suggesting that HDAC failed to interact with GFP/CID/SM/CIMmt. Therefore, HDAC could bind to both the SM and the CIM in the CID.

Expression of MEL1S with double mutants of SM and CIM in L-G3 cells did not block granulocyte differentiation induced by G-CSF

Finally, to determine whether the combined repressor activity by sumoylation and CtBP-binding ability might be related to the differentiation blockade by MEL1S, a MEL1S expression vector containing SMmt and CIMmt (SM/CIMmt) was constructed and transfected into L-G3 cells. After the establishment of the MEL1S/SM/

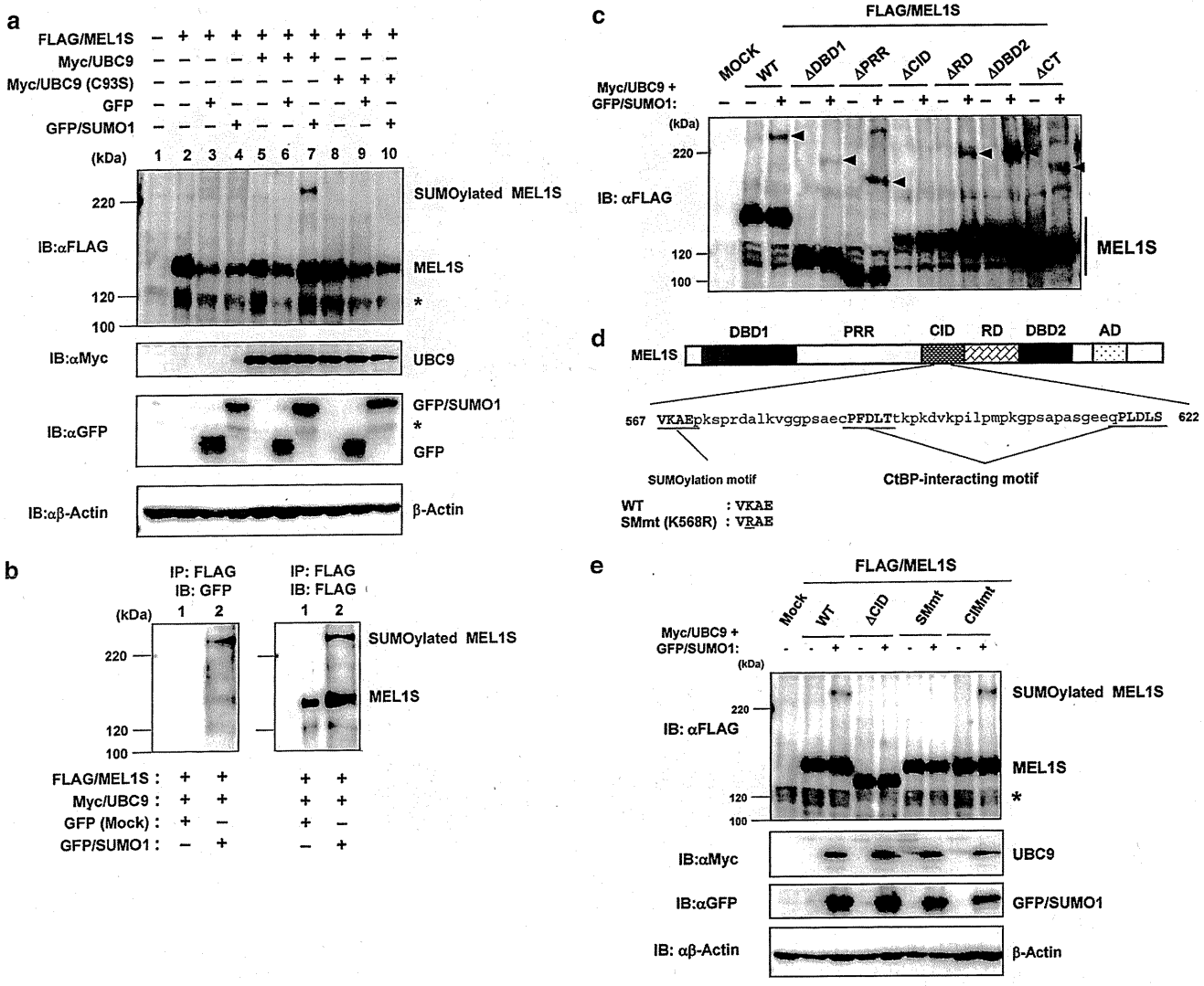

Figure 4 MEL1S was sumoylated at lysine 568 in a SM adjacent to the CIM. (**a**) Sumoylation of MEL1S is dependent on UBC9. Cells (293T) were co-transfected with expression plasmids encoding FLAG/MEL1S, Myc-tagged UBC9 or Myc-tagged dominant negative UBC9 (the C93S mutant) and/or GFP/SUMO1. The cell lysates were analyzed by western blotting using an anti-FLAG antibody. Expression of UBC9, SUMO1 and β-Actin is shown in the three lower panels. Molecular weight markers are given in kDa. (**b**) Identification of sumoylated MEL1S by immunoblot analysis. Flag-tagged MEL1S with Myc/UBC9 was transfected along with control GFP or GFP-fused SUMO1 into 293T cells. After immunoprecipitation with an anti-FLAG antibody, sumoylated MEL1S was detected using an anti-GFP antibody for GFP/SUMO1 in the left panel. In the right panel, after immunoprecipitation out of the same samples with the anti-FLAG antibody, MEL1S was identified using an anti-FLAG antibody. (**c**) The detection of the more slowly migrating band of MEL1S as a sumoylated form of MEL1S by transfection of expression vectors containing each MEL1S mutant is indicated in Figure 2a, with or without Myc/UBC9 and GFP/SUMO1 expression plasmids. Cells (293T) were transfected under the same conditions as in Figure 4a, and the cell lysates were analyzed by western blotting using an anti-FLAG antibody. Molecular weight markers are given in kDa. Stars indicate sumoylated MEL1S. (**d**) Schematic illustration of human MEL1S and the mutant form of MEL1S. MEL1S has a SM (VKAE) adjacent to two CIMs (PFDLT and PLDLS). These motifs are located in the CID of MEL1S. The SM was mutated to VRAE by site-directed mutagenesis. Abbreviations are the same as in Figure 3a. (**e**) The MEL1S K568R mutant cannot be sumoylated. An expression plasmid encoding either FLAG/MEL1S (WT), the CID-deleted MEL1S mutant (ΔCID), the SM-abolished mutant (SMmt) or the CIM-abolished mutant (CIMmt) was transfected with or without Myc/UBC9 and GFP/SUMO1 expression plasmids into 293T cells, and the cell lysates were analyzed by western blotting using an anti-FLAG antibody. Expression of UBC9, SUMO1 and β-Actin is shown in the three lower panels.

CIMmt #1 and #2 cell lines (Figure 3c), a series of L-G3 cell lines expressing WT or mutant MEL1S were cultured with a vehicle, IL-3 or G-CSF for 6 days. The major difference between the control and MEL1S/SM/CIMmt cell lines was the different patterns of cell growth in cultures supplemented with G-CSF. In response to G-CSF, parental and L-G3/Mock control cells grew slowly and differentiated into granulocytes, but L-G3 cells with MEL1S or MEL1S/CIMmt expression grew without differentiating into granulocytes (Figures 7a and b). The patterns of cell growth in the two MEL1S/SM/CIMmt cell lines were very similar to those of the parental and L-G3/Mock cell lines, and both MEL1S/SM/CIMmt cell lines showed granulocyte

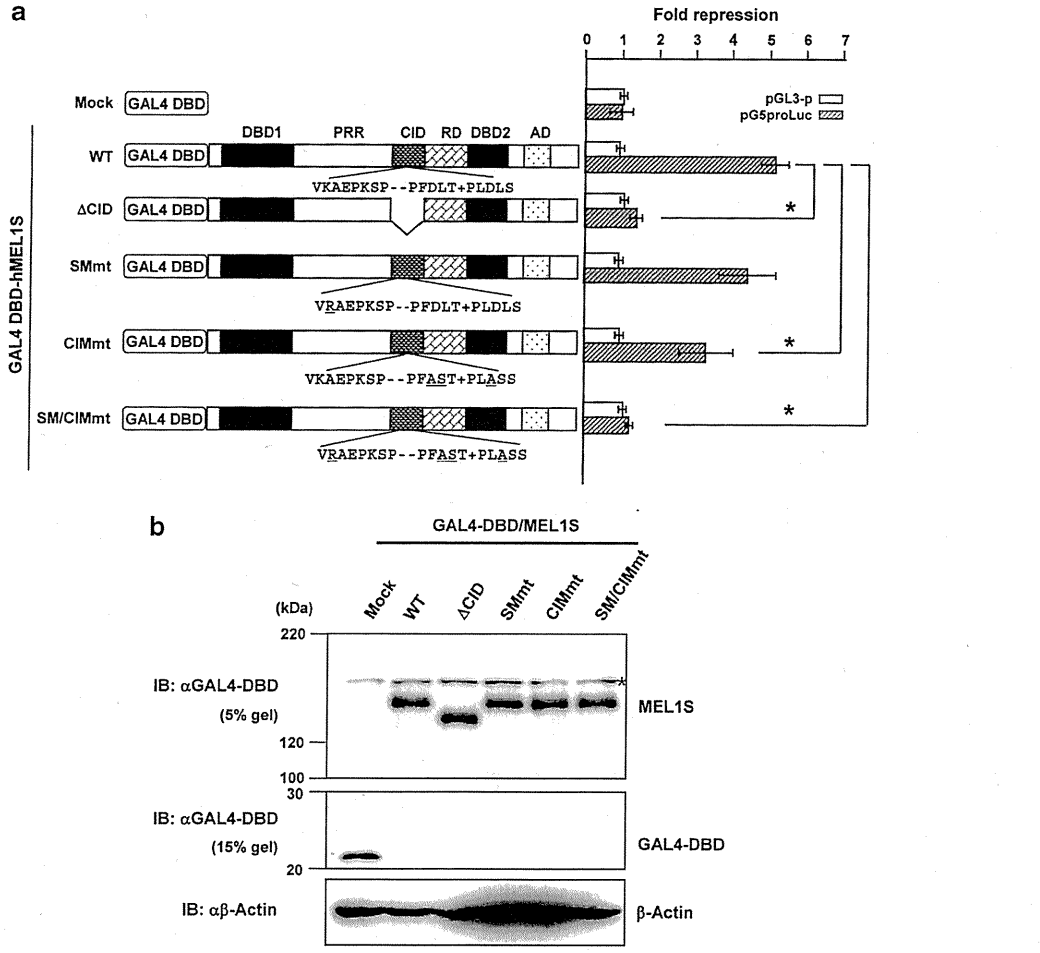

Figure 5 Mutation of both the SM and the CIMs in MEL1S abolishes its transcriptional repressor activity. (**a**) Transcriptional repressor activities of GAL4–DBD-fused MEL1S and mutant forms of MEL1S. COS-7 cells were co-transfected with the luciferase reporter vector (pGL3-p or pG5proLuc) and an internal control plasmid, pRL-MP, along with an expression vector for GAL4–DBD/MEL1S or its mutants, as illustrated in Figure 5a. The reporter assay was carried out 48 h after transfection. Values of relative luciferase activity represent the mean ± s.d. of three independent transfections. $*P<0.05$ (Student's *t*-test). (**b**) The protein expression levels of transfected MEL1S and the deletion mutants in COS-7 cells were determined by western blotting using the anti-GAL4-DBD antibody. The star indicates a nonspecific band.

differentiation with multi-lobulated nuclei after 6 days of culture with G-CSF. To confirm granulocyte differentiation, the expression of *MPO* and *Lf* in these cells was analyzed 6 days after treatment with G-CSF by reverse-transcription–PCR (Figure 7d). The expression of *MPO* and *Lf* was detected in parental, Mock and MEL1S/SM/CIMmt #1 and #2 cells. The lower level of *MPO* expression in the MEL1S/SM/CIMmt cells may reflect the presence of a small number of immature myeloid cells (Figures 7c). To confirm the results, these experiments were repeated in the IL-3-dependent murine myeloid cell line 32Dcl3 expressing either WT MEL1S or MEL1S/SM/CIMmt. The forced expression of WT MEL1S was found, but MEL1S/SM/CIMmt did not result in the inhibition of G-CSF-induced differentiation in 32Dcl3 cells (Supplementary Figures 2a, b, c, d and e). To confirm whether MEL1S was sumoylated in L-G3 cells, stable -L-G3 cell lines expressing WT or mutant MEL1S were transfected with Myc/UBC9 and GFP/SUMO1 expression plasmids, and sumoylation levels were determined by western blot analysis with the anti-FLAG antibody. A slowly migrating band corresponded to sumoylated MEL1S and was detected in the lysates from MEL1S/WT and MEL1S/CIM cells but not from MEL1S/SM/CIMmt #1 or #2 cells (Figure 7e). These data suggest that the ability of MEL1S to block differentiation was primarily dependent on the transcriptional repression activity mediated by both sumoylation and CtBP binding in the CID of MEL1S.

Discussion

In this study, we showed that sumoylation of and CtBP interaction with the CID cooperatively mediated transcriptional repression activity of the MEL1 zinc-finger protein; in addition, MEL1 transcriptional repression activity was found to be essential for its blockade of G-CSF-induced granulocyte differentiation of

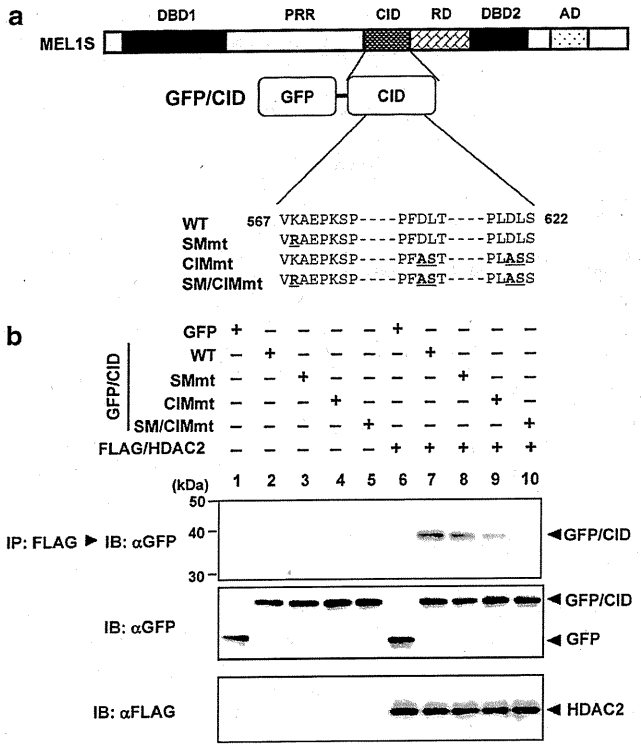

Figure 6 Mutation of both the SM and the CIMs abolishes the recruitment of HDAC2 to the CID of MEL1S. (**a**) Schematic illustration of human MEL1S and GFP-fused CID. Amino-acid substitutions in the SM and/or the CIM are shown at the bottom. Abbreviations are the same as those in Figure 3a. (**b**) Neither the SM nor the CIM-disrupted CID can interact with HDAC2. Either a GFP/CID fusion (WT, SMmt, CIMmt, SM/CIMmt) vector or the mock (GFP) vector was co-transfected with or without a vector expressing FLAG/HDAC2 into 293T cells. The cell lysates were subjected to immunoprecipitation with the anti-FLAG antibody and blotted with an anti-GFP antibody. WT GFP/CID and the three mutant forms that interacted with HDAC2 are shown in the top panel. The direct western blotting of CID using the anti-GFP antibody and of HDAC2 using the anti-FLAG antibody are shown in the middle and bottom panels, respectively.

murine IL-3-dependent L-G3 cells. We have identified an important SUMO acceptor site at lysine 568, which lies just adjacent to the CIM, within the CID. Amino-acid substitutions in the SM and CIM of MEL1S completely abrogated the protein's transcriptional repression activity and its recruitment of the HDAC complex. Finally, L-G3 cells were stably transfected with a double mutant of MEL1S (SM/CIMmt) and differentiated into granulocytes on treatment with G-CSF. Although the sumoylation status of MEL1S has not been shown in acute myeloid leukemia cells, these data demonstrate that the overexpression of MEL1 in a myeloid cell line could inhibit G-CSF-induced granulocyte differentiation through transcriptional repression of yet unidentified genes, and this pathway may contribute to myeloid leukemogenesis.

Several C_2H_2 zinc-finger transcription factors contain CIM and SM that have an important role in modulating transcriptional repressor activity. BKLF, a Krüppel-like C_2H_2 zinc-finger transcription factor expressed in erythroid cells, contains a CIM and two SMs (Perdomo *et al.*, 2005). The SUMO site at K10 resides in the repression domain and is located 41 amino-acids upstream from the CIM, and the other SUMO site (K198) is located between the repressor domain and the zinc-finger DBD (Perdomo *et al.*, 2005). Sumoylation and interaction with CtBP synergistically enhanced the transcriptional repression activity of BKLF (Perdomo *et al.*, 2005). Both ZEB1 and ZEB2 have been reported to be sumoylated on two conserved lysine residues; one SUMO site (K774 in ZEB1 and K866 in ZEB2) is located adjacent to a CIM, and another site (K347 in ZEB1 and K391 in ZEB2) is located between the first zinc-finger cluster (composed of zinc-finger repeats 1–4) and the Smad-binding domain. Mutations of these two sumoylated lysine residues in ZEB1 caused a loss of the transcriptional repression function of ZEB1, and the DNA binding ability of ZEB1 was shown to be dependent on the sumoylation of the two lysine residues in a chromatin immunoprecipitation assay (Kuppuswamy *et al.*, 2008). Conversely, the sumoylation of ZEB2 attenuates its transcriptional repression of E-cadherin, which is caused by reduced binding to the co-repressor CtBP (Long *et al.*, 2005). Although the function of sumoylation of zinc-finger transcription factors with CIM differs from one transcription factor to the next, sumoylation of the BKLF and MEL1S transcription factors may facilitate recruitment of the HDAC complex to increase transcriptional repression activity; however, a study of BKLF did not show an increased recruitment of the HDAC complex upon sumoylation (Perdomo *et al.*, 2005).

Hematopoietic cell differentiation is regulated by lineage-specific transcription factors that function in a mutually antagonistic manner. For example, MafB and c-Myb function as antagonists for each other in a balance between macrophage differentiation and myeloid progenitor expansion. C-Myb suppresses MafB-driven differentiation through sumoylation of MafB (Tillmanns *et al.*, 2007); conversely, c-Myb is also affected by sumoylation. TRAF7, a SUMO ligase, sequesters c-Myb in the cytoplasm by increasing its sumoylation (Morita *et al.*, 2005). Thus, sumoylation is one of the important regulatory events in cellular differentiation and proliferation. Interestingly, MEL1/PRDM16 is one of transcription factors in the regulation of brown fat versus white fat/skeletal muscle differentiation (Seale *et al.*, 2008). In myoblasts and preadipocytes, MEL1/PRDM16 promotes the expression of brown fat cell-selective genes by co-activating the transcriptional activity of PGC-1α/1β and PPARα/γ through direct interaction (Kajimura *et al.*, 2008). In addition, MEL1/PRDM16 represses the expression of white fat- or skeletal muscle-specific genes by association with the co-repressor CtBP (Kajimura *et al.*, 2009). Although the mechanisms underlying the molecular switch that changes MEL1/PRDM16 from a transcriptional activator to a repressor have not yet been elucidated, sumoylation may have an important role in this transcriptional switch. Given that the overexpression of MEL1S was found to block the granulocytic

differentiation of L-G3 myeloid leukemia cells, inhibition of MEL1S sumoylation through targeting of tissue-specific SUMO ligases may present a novel strategy in myeloid leukemia. The SUMO ligases for MEL1S in hematopoietic stem cells and/or myeloid progenitor cells remain to be identified.

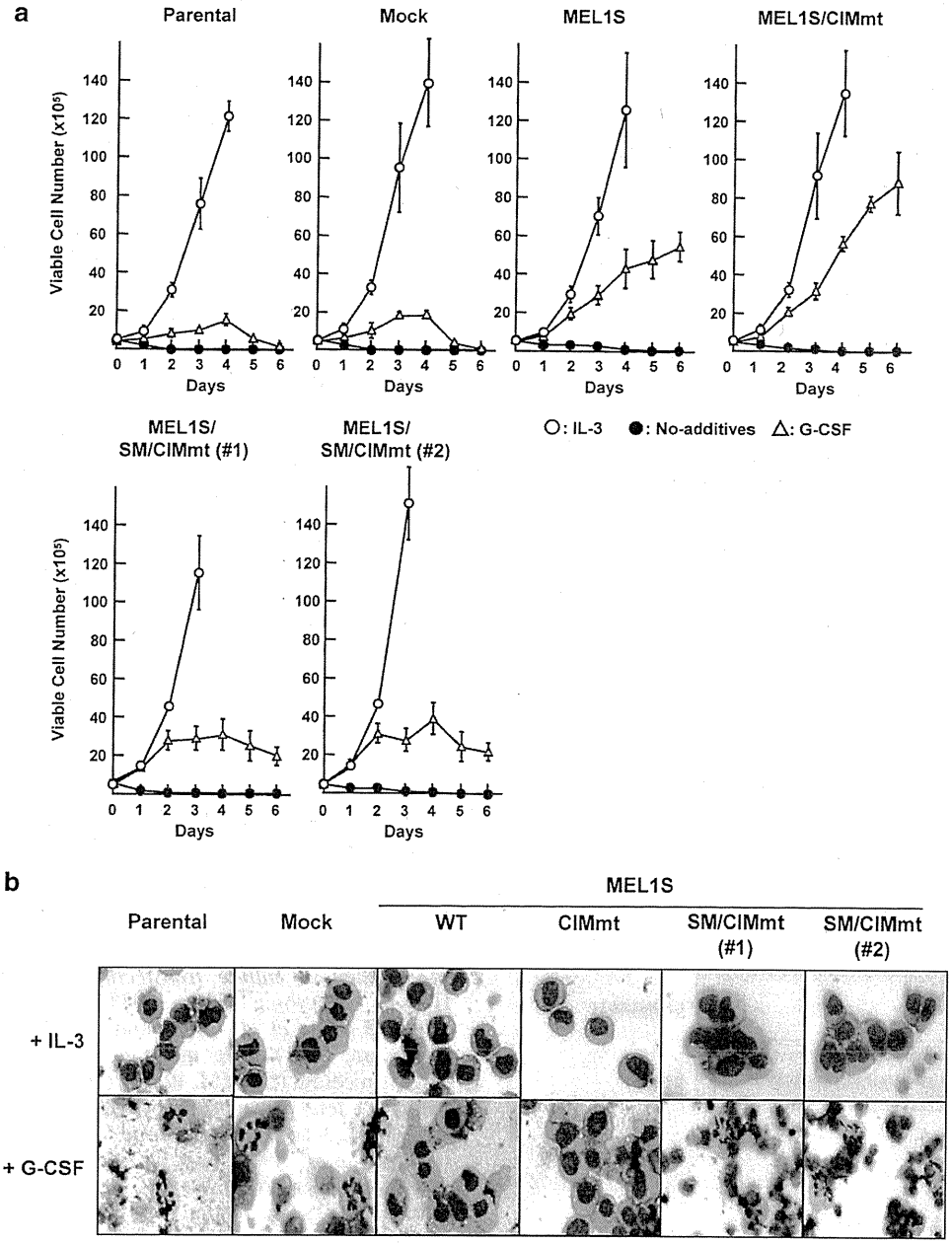

Figure 7 L-G3 transformants overexpressing SM and/or CIM motif-disrupted MEL1S mutants differentiate into granulocytes in response to G-CSF. (**a**) Growth curves of L-G3 cells infected with retrovirus with *MEL1S* mutants lacking a SM or two CIMs. L-G3 cells stably expressing either FLAG-tagged MEL1S (L-G3/MEL1S), the CtBP interaction mutant (L-G3/MEL1S/CIMmt), the mutant with both the SM and the CIMs disrupted (L-G3/MEL1S/SM/CIMmt, #1 and #2, corresponding to lanes 7 and 8 in Figure 3c) or the mock vector (L-G3/Mock) and the parental cells were grown under different culture conditions. Viable cells were counted using the trypan-blue exclusion method at each time point. Open or closed circles indicate the culture conditions using medium with or without IL-3, respectively, and open triangles indicate medium with G-CSF. The error bars represent the s.d. of three independent experiments. (**b**) May-Grünwald-Giemsa staining was performed on parental and infected L-G3 cells after cultivation in medium containing IL-3 (top panel) or G-CSF (bottom panel) for 6 days. Pictures were taken at × 100 magnification. (**c**) Comparison of cell populations among various transformants of L-G3 cells estimated by counting stained nuclei after 6 days of culture in medium with G-CSF. The data show the results from two independent experiments and are presented as in Figure 1c. (**d**) Semi-quantitative RT–PCR assessment of *Mpo* and *Lf* mRNA levels was performed on RNA isolated from cells cultured in medium with IL-3 or G-CSF for 6 days. (**e**) The MEL1S in the L-G3 transformants was sumoylated. The transient transfection of Myc/UBC9 and GFP/SUMO1 expression plasmids into L-G3 transformants was performed by Amaxa Nucleofection systems (Wako), and the cell lysates were analyzed by western blotting using an anti-FLAG antibody. The expression of UBC9, SUMO1 and β-Actin is shown in the three lower panels.

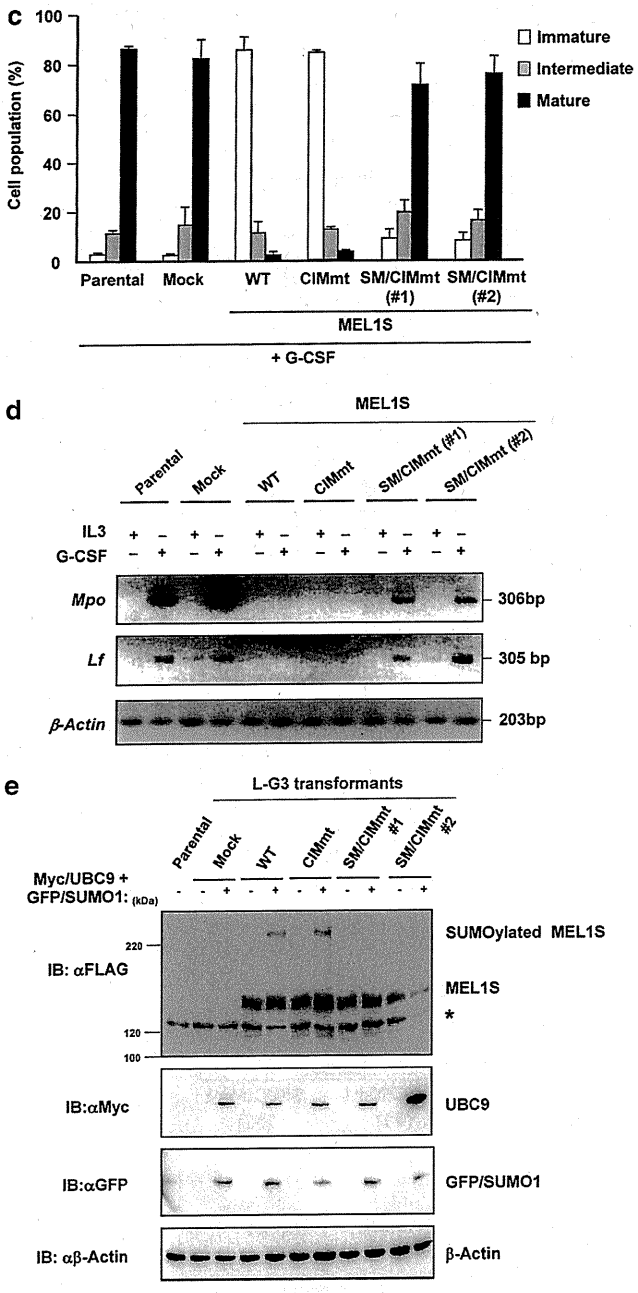

Figure 7 Continued.

Materials and methods

Plasmid constructions

To construct human *MEL1S* expression vectors, a FLAG- or a hemagglutinin (HA)-epitope tagged, short-form MEL1 lacking an *N*-terminal PR domain (*MEL1S*) (Mochizuki *et al*., 2000; Nishikata *et al*., 2003) was placed under the control of a cytomegalovirus (CMV) promoter in a mammalian expression vector pCMV26 (Sigma-Aldrich, St Louis, MO, USA) (pFLAG-MEL1S or pHA-MEL1S). To construct the human *MEL1* expression vector, a HA-epitope tagged, long-form MEL1 with a PR domain (Mochizuki *et al*., 2000; Nishikata *et al*., 2003) was inserted into the pCMV26 (pHA-MEL1). Using the In-Fusion cloning kit (Clontech, Mountain View, CA, USA), deletion mutants of MEL1S, including MEL1S/ΔDBD1 (DBD1, containing the 1–7 zinc-finger repeats, aa 40–264), MEL1S/ΔPRR (proline-rich region, aa 265–522), MEL1S/ΔCID (CID, aa 523–644), MEL1S/ΔRD (repression domain, aa 645–766), MEL1S/ΔDBD2 (DBD2, containing the 8–10 zinc-finger repeats, aa 767–887) and MEL1S/ΔCT (*C*-terminal region containing acidic domain, aa 893–1072), were generated by PCR amplification of human *MEL1S* complementary DNA lacking each domain structure (Figure 2a). To generate MEL1S mutants with amino-acid substitutions, a mutant with lysine 568 replaced by arginine in the SM (MEL1S/SMmt with K568R), the CIM mutant MEL1S-CIMmt (PFAST at aa 588-592 and PLASS at aa 618-622), and the double mutant (MEL1S/SM/CIMmt) were generated using a Quick Change II site-directed mutagenesis kit (Stratagene, La Jolla, CA, USA). The GAL4 DBD-fused MEL1S expression constructs with various deletions and amino acid replacements were cloned into the pM expression vector (Clontech). The murine CtBP2 expression vector, pFLAG-CtBP2, contained a full-length murine *CtBP2* (kindly provided by Dr Crossley; Turner and Crossley, 1998) cloned into the FLAG-epitope tag expression vector pFLAG-Mock. The human UBC9 expression vectors, pMyc-UBC9 and pMyc-UBC9DN, contain full-length human *UBC9* and the dominant negative mutant (C93S), respectively, cloned into the Myc-epitope tag expression vector pMyc-Mock. The human SUMO expression vector pGFP-SUMO1 contains full-length human *SUMO-1* and was cloned into the pGFP-epitope tag expression vector pGFP-Mock. A series of CID fragments from MEL1S containing WT CID (CID/WT) or CID with a series of amino-acid substitutions (CID/SMmt, CID/CIMmt and CID/SM/CIMmt) were cloned into the pGFP-epitope tag expression vector pGFP-Mock. The chicken HDAC2 expression vector pFLAG-HDAC2 and the Mock vector were kindly provided by Dr Y Takami (University of Miyazaki, Miyazaki, Japan). For the reporter gene assay, the pG5proLuc vector was used as a reporter expressing firefly luciferase (Nishikata *et al*., 2003). The TK promoter in the pG4.74 *Renilla* luciferase internal control vector (Promega, Madison, WI, USA) was replaced with the minimum promoter (MP) from the pGL4.23 firefly luciferase reporter vector (Promega) to generate pRL-MP.

Mammalian cell culture, transfection and infection

Human embryonic kidney 293T (DuBridge *et al*., 1987), BOSC23 (Pear *et al*., 1993) and simian kidney COS-7 cells (Gluzman, 1981) were maintained in Dulbecco's modified Eagle's medium (DMEM, Wako, Osaka, Japan) supplemented with 10% fetal bovine serum (FBS, Biofluids, Camarillo, CA, USA). IL-3-dependent murine myeloid cell lines, L-G3 (Kinashi *et al*., 1991) and 32Dcl3 (Greenberger *et al*., 1983; Migliaccio *et al*., 1989) were maintained in RPMI 1640 (Wako) with 10% FBS and 5 ng/ml murine IL-3 (mIL-3, Kirin Brewery Co., Tokyo, Japan). The cells were grown in 5% CO_2 at 37 °C. Transfections were carried out using the Hilymax transfection reagent (DOJINDO, Kumamoto, Japan), according to the manufacturer's instructions. Transfection studies of L-G3 transformants for sumoylation assays and of 32Dcl3 cells for the generation of stable transformants were carried out using the Amaxa Nucleofection systems (Wako), according to the manufacturer's instructions. Cells were harvested 48 h after transfection for further analysis.

Retroviral infections

To generate L-G3 clones stably expressing WT human MEL1S and two of its mutants (MEL1S/CIMmt and MEL1S/SM/CIMmt), the respective complementary DNA sequences

were subcloned into the retroviral vector pLXSN (Clontech). Infectious retroviral particles bearing FLAG-tagged MEL1S/WT, MEL1S/CIMmt, or MEL1S/SM/CIMmt were prepared by transfection of the virus-producing BOSC23 cells with each retroviral expression vector. Neomycin-resistant clones were screened for expression of the FLAG-tagged proteins by immunoblot analysis using an anti-FLAG rabbit polyclonal antibody (Sigma-Aldrich).

Proliferation and differentiation assays

The L-G3 or 32Dcl3 stable cell lines were seeded at 1×10^5 cells/well in a 6-well dish and incubated for 24 h. The cells were subsequently washed twice in RPMI 1640 and incubated with 5 ng/ml mIL-3, 5 ng/ml G-CSF, 5 ng/ml G-CSF and 3 ng/ml TSA (Wako) or no growth factor for 6 (L-G3) or 9 days (32Dcl3). The morphological observations were studied by cytospinning the cells onto glass slides and staining with May-Grünwald-Giemsa solution (Merck, Darmstadt, Germany). For the measurement of viable cell numbers, live cells were counted at indicated intervals using trypan blue exclusion (Sigma-Aldrich). Murine IL-3 and G-CSF were kindly provided by Kirin Brewery Co. All results were reproduced twice.

Immunoprecipitation and immunoblot analyses

Transfected cells were directly lysed in SDS sample buffer, boiled, resolved on 5 or 10% SDS–polyacrylamide gels, and transferred to polyvinylidene fluoride (PVDF) membranes (Immobilon-P, Millipore, Billerica, MA, USA). For immunoprecipitation assays, 5×10^6 cells were washed in phosphate-buffered saline and solubilized with 450 µl of radioimmune precipitation assay (RIPA) buffer (50 mM Tris-HCl, pH 7.5, 150 mM NaCl, 5 mM EDTA, and 1% Triton X-100), which was supplemented with a protease inhibitor cocktail (Sigma-Aldrich). After centrifugation, the supernatants were incubated with 50 µl of anti-Flag M2 affinity gel (Sigma-Aldrich) overnight with rotation at 4 °C. The resins were washed three times with RIPA buffer, and proteins were eluted in SDS sample buffer. The detection of FLAG-, HA-, Myc- and GFP-tagged proteins was carried out using rabbit anti-Flag (1:1000, Sigma-Aldrich), rat monoclonal anti-HA (1:1000, 3F10, Roche, Manheim, Germany), mouse monoclonal anti-Myc (1:1000, 9B11, Cell Signaling Technology, Danvers, MA, USA) and rabbit anti-GFP (1:1000, MBL, Nagoya, Japan) antibodies. Mouse monoclonal anti-GAL4 DNA-BD (1:2000, Clontech), rabbit anti-MEL1 DBD1 (1–7 zinc-finger cluster) and DBD2 (8–10 zinc-finger cluster, 1:1000) antibodies (Nishikata *et al.*, 2003) were also used, and a mouse monoclonal anti-β-Actin antibody (1:5000, AC15, Sigma-Aldrich) was used to provide an internal loading control. Horseradish peroxidase-linked swine anti-rabbit, rabbit anti-rat (DakoCytomation Denmark A/S, Glostrup, Denmark), and sheep anti-mouse (GE Healthcare, Little Chalfont, England) immunoglobulins were used as secondary antibodies. Immunoreactive proteins were visualized on LAS-3000 (Fuji-film, Tokyo, Japan) using a Lumi-Light Plus western blotting substrate (Roche). All results were reproduced twice.

Reverse-transcriptase–PCR

Total RNA was extracted from each cell using Trizol reagents (Invitrogen, Carlsbad, CA, USA) and converted to complementary DNA using AMV reverse transcriptase (Takara, Shiga, Japan). The complementary DNA was used as a template for PCR performed by ExTaq polymerase (Takara), and the primers used were as follows: for mouse *Mpo*, forward 5′-CGCTTCTCCTTCTTCACTGG-3′ and reverse 5′-CTGCC ATTGTCTTGGAATCG-3′; for mouse *Lf*, forward 5′-AAAC AAGCATCGGGATTCCAG-3′ and reverse 5′-ACAATGC AGTCTTCCGTGGTG-3′; and for mouse *β-Actin*, forward 5′-TTCCTTCTTGGGTATGGAAT-3′ and reverse 5′-GAGC AATGATCTTGATCTTC-3′.

Reporter gene assay

Reporter gene assays were carried out using a GAL4-responsive artificial promoter-luciferase plasmid (pG5proLuc) (Nishikata *et al.*, 2003). Briefly, COS-7 cells were transfected in 12-well plates with 2 µg of DNA, which included the indicated reporter constructs and expression vectors, as well as 100 ng of pRL-MP plasmid as an indicator of transfection efficiency. The luciferase activities (firefly luciferase for the reporter and *Renilla* luciferase for the indicator) were measured using the Dual-Luciferase Assay System (Promega). All transfections were carried out in triplicate. The data obtained were compared with the control and statistically analyzed by Student's *t*-test.

Conflict of interest

The authors declare no conflict of interest.

Acknowledgements

This work was supported in part by Grants-in-Aid for Scientific Research of Priority Area from the Ministry of Education, Culture, Sports, Science and Technology in Japan.

References

Bloomfield CD, Garson OM, Volin L, Knuutila S, de la Chapelle A. (1985). t(1;3)(p36;q21) in acute nonlymphocytic leukemia: a new cytogenic-clinicopathologic association. *Blood* **66**: 1409–1413.

Chinnadurai G. (2007). Transcriptional regulation by C-terminal binding proteins. *Int J Biochem Cell Biol* **39**: 1593–1607.

DuBridge RB, Tang P, Hsia HC, Phai-Mooi L, Miller JH, Calos MP. (1987). Analysis of mutation in human cells by using Epstein-Barr virus shuttle system. *Mol Cell Biol* **7**: 379–387.

Friedman AD, Krieder BL, Venturelli D, Rovera G. (1991). Transcriptional regulation of two myeloid-specific genes, myeloperoxidase and lactoferrin, during differentiation of the murine cell line 32Dcl3. *Blood* **78**: 2426–2432.

Giorgino F, de Robertis O, Laviola L, Montrone C, Perrini S, McCowen K *et al.* (2000). The sentrin-conjugating enzyme mUBC9 interacts with transient transfection GLUT4 and GLUT1 glucose transporters and regulates transporter levels in skeletal muscle cells. *Proc Natl Acad Sci USA* **97**: 1125–1130.

Gluzman Y. (1981). SV40-transformed simian cells support the replication of early SV40 mutants. *Cell* **23**: 175–182.

Greenberger JS, Sakakeeny MA, Humphries RK, Eaves CJ, Eckner RJ. (1983). Demonstration of permanent factor-dependent multipotential (erythroid/neutrophil/basophil) hematopoietic progenitor cell line. *Proc Natl Acad Sci USA* **80**: 2931–2935.

Izutsu K, Kurokawa M, Imai Y, Maki K, Mitani K, Hirai H. (2001). The corepressor CtBP interacts with Evi-1 to repress transforming growth factor beta signaling. *Blood* **97**: 2815–2822.

Kagey MH, Melhuish TA, Wotton D. (2003). The polycomb protein Pc2 is a SUMO E3. *Cell* **113**: 127–137.

Kajimura S, Seale P, Kubota K, Lunsford E, Frangioni JV, Gygi SP *et al.* (2009). Initiation of myoblast to brown fat switch by a PRDM16-C/EBP-b transcriptional complex. *Nature* **460**: 1154–1159.

Kajimura S, Seale P, Tomaru T, Erdjument-Bromage H, Cooper MP, Ruas JL *et al.* (2008). Regulation of the brown and white fat gene programs through a PRDM16/CtBP transcriptional complex. *Genes Dev* **22**: 1397–1409.

Kinashi T, Lee HL, Ogawa M, Tohyama K, Tashiro K, Fukunaga R *et al.* (1991). Premature expression of the macrophage colony-stimulating factor receptor on a multipotential stem cell line does not alter differentiation lineages controlled by stromal cells used for coculture. *J Exp Med* **173**: 1267–1279.

Kuppuswamy M, Vijayalingam S, Zhao LJ, Zhou Y, Subramanian T, Ryerse J *et al.* (2008). Role of the PLDLS-binding cleft region of CtBP1 in recruitment of core and auxiliary components of the corepressor complex. *Mol Cell Biol* **28**: 269–281.

Long J, Zuo D, Park M. (2005). Pc2-mediated SUMOylation of Smad-interacting protein 1 attenuates transcriptional repression of E-cadherin. *J Biol Chem* **280**: 35477–35489.

Maki K, Yamagata T, Mitani K. (2008). Role of the *RUNX1-EVI1* fusion gene in leukemogenesis. *Cancer Sci* **99**: 1878–1883.

Migliaccio G, Migliaccio AR, Kreider BL, Rovera G, Adamson JW. (1989). Transcriptional regulation of two myeloid-specific genes, myeloperoxidase and lactoferrin, during differentiation of the murine cell line 32D C13. *J Cell Biol* **109**: 833–841.

Mitani K. (2004). Molecular mechanisms of leukemogenesis by AML1/EVI-1. *Oncogene* **23**: 4263–4269.

Mochizuki N, Shimizu S, Nagasawa T, Tanaka H, Taniwaki M, Yokota J *et al.* (2000). A novel gene, *MEL1*, mapped to 1p36.3 is highly homologous to the *MDS1/EVI1* gene and is transcriptionally activated in t(1;3)(p36;q21)-positive leukemia cells. *Blood* **96**: 3209–3214.

Moir DJ, Jones PAE, Pearson J, Ducan JR, Cook P, Buckle VJ. (1984). A new translocation, t(1;3)(p36;q21), in myelodysplastic disorders. *Blood* **64**: 553–555.

Morishita K. (2007). Leukemogenesis of the EVI1/MEL1 gene family. *Int J Hematol* **85**: 279–286.

Morita Y, Kanei-Ishii C, Nomura T, Ishii S. (2005). TRAF7 sequesters c-Myb to the cytoplasm by stimulating its SUMOylation. *Mol Biol Cell* **16**: 5433–5444.

Nishikata I, Sasaki H, Iga M, Tateno Y, Imayoshi S, Asou N *et al.* (2003). A novel EVI1 gene family, *MEL1*, lacking a PR domain (MEL1S) is expressed mainly in t(1;3)(p36;q21)-positive AML and blocks G-CSF-induced myeloid differentiation. *Blood* **102**: 3323–3332.

Pear WS, Nolan GP, Scott ML, Baltimore D. (1993). Production of high-titer helper-free retroviruses by transient transfection. *Proc Natl Acad Sci USA* **90**: 8392–8396.

Perdomo J, Verger A, Turner J, Crossley M. (2005). Role for SUMO modification in facilitating transcriptional repression by BKLF. *Mol Cell Biol* **25**: 1549–1559.

Quinlan KGR, Nardini M, Verger A, Francescato P, Yaswen P, Corda D *et al.* (2006). Specific recognition of ZNF217 and other zinc finger proteins at a surface groove of C-terminal binding proteins. *Mol Cell Biol* **26**: 8159–8172.

Rodriguez MS, Dargemont C, Hay RT. (2001). SUMO-1 conjugation *in vivo* requires both a consensus modification motif and nuclear targeting. *J Biol Chem* **276**: 12654–12659.

Schaeper U, Boyd JM, Verma S, Uhlmann E, Subramanian T, Chinnadurai G. (1995). Molecular cloning and characterization of a cellular phosphorprotein that interacts with a conserved C-terminal domain of adenovirus E1A involved in negative modulation of oncogenic transformation. *Proc Natl Acad Sci USA* **92**: 10467–10471.

Seale P, Bjok B, Yang W, Kajimura S, Chin S, Kuang S *et al.* (2008). PRDM16 controls a brown fat/skeletal muscle switch. *Nature* **454**: 961–967.

Shimahara A, Yamakawa N, Nishikata I, Morishita K. (2010). Acetylation of lysine 564 Adjacent to the C-terminal binding protein-binding motif in EVI1 is crucial for transcriptional activation of *GATA2*. *J Biol Chem* **285**: 16967–16977.

Shimizu S, Suzukawa K, Kodera T, Nagasawa T, Abe T, Taniwaki M *et al.* (2000). Identification of breakpoint cluster regions at 1p36.3 and 3q21 in hematologic malignancies with t(1;3)(p36;q21). *Genes Chromosomes Cancer* **27**: 229–238.

Tillmanns S, Otto C, Jaffray E, Roure CD, Bakri Y, Vanhille L *et al.* (2007). SUMO modification regulates MafB-driven macrophage differentiation by enabling Myb-dependent transcriptional repression. *Mol Cell Biol* **27**: 5554–5564.

Turner J, Crossley M. (1998). Cloning and characterization of mCtBP2, a co-repressor that associates with basic Krüppel-like factor and other mammalian transcriptional regulators. *EMBO J* **17**: 5129–5140.

Welborn JL, Lewis JP, Jenks H, Walling P. (1987). Diagnostic and prognostic signification of t(1;3)(p36;q21) in the disorders of hematopoiesis. *Cancer Genet Cytogenet* **28**: 277–285.

Supplementary Information accompanies the paper on the Oncogene website (http://www.nature.com/onc)

Leukemia (2011) 25, 921–931

www.nature.com/leu

ORIGINAL ARTICLE

CD52 as a molecular target for immunotherapy to treat acute myeloid leukemia with high EVI1 expression

Y Saito, S Nakahata, N Yamakawa, K Kaneda, E Ichihara, A Suekane and K Morishita

Department of Medical Science, Division of Tumor and Cellular Biochemistry, Faculty of Medicine, University of Miyazaki, Miyazaki, Japan

Ecotropic viral integration site 1 (EVI1) is an oncogenic transcription factor in human acute myeloid leukemia (AML) with chromosomal alterations at 3q26. Because a high expression of EVI1 protein in AML cells predicts resistance to chemotherapy with a poor outcome, we have searched for molecular targets that will treat these patients with AML. In this study, we determined that CD52, which is mainly expressed on lymphocytes, is highly expressed in most cases of AML with a high EVI1 expression (EVI1^{High}). CAMPATH-1H, a humanized monoclonal antibody against CD52, has been used to prevent graft-versus-host disease and treat CD52-positive lymphoproliferative disorders. Here, we investigated the antitumor effect of CAMPATH-1H on EVI1^{High} AML cells. CAMPATH-1H significantly inhibited cell growth and induced apoptosis in CD52-positive EVI1^{High} leukemia cells. Furthermore, CAMPATH-1H induced complement-dependent cytotoxicity and antibody-dependent cellular cytotoxicity against CD52-positive EVI1^{High} leukemia cells. After an intravenous injection of CAMPATH-1H into NOD/Shi-scid/IL-2Rγ;null mice with subcutaneous engraftment of EVI1^{High} leukemia cells, tumor growth rates were significantly reduced, and the mice survived longer than those in the phosphate-buffered saline-injected control group. Thus, CAMPATH-1H is a potential therapeutic antibody for the treatment of patients with EVI1^{High} leukemia.
Leukemia (2011) **25,** 921–931; doi:10.1038/leu.2011.36;
published online 11 March 2011
Keywords: CD52; CAMPATH-1H; EVI1; acute myeloid leukemia

Introduction

Murine ecotropic viral integration site 1 (EVI1) was first identified as a leukemia-associated gene activated by murine retroviral integration.[1,2] A high expression of the human homologue EVI1 is found in 5–10% of patients with acute myeloid leukemia (AML), but chromosome 3q26 abnormalities near the *EVI1* gene are only detected in 1–3% of all AML cases.[3–5] Because AML patients with a high EVI1 expression (EVI1^{High}) had a significantly reduced overall survival, overexpression of the *EVI1* gene is thought to be a poor prognostic factor for AML patients.[6,7] Patients with EVI1^{High} AML often do not respond to chemotherapy and hematopoietic cell transplantation;[8] therefore, identifying novel molecular targets in EVI1^{High} AML is of particular importance. In this study, we identified CD52 as a new surface molecule highly expressed on most EVI1^{High} leukemia cells by DNA microarray, reverse-transcription polymerase chain reaction (RT-PCR) and flow cytometry analyses.

Correspondence: Dr K Morishita, Division of Tumor and Cellular Biochemistry, Department of Medical Science, Faculty of Medicine, University of Miyazaki, 5200 Kihara, Kiyotake-cho, Miyazaki 889-1692, Japan.
E-mail: kmorishi@med.miyazaki-u.ac.jp
Received 11 October 2010; revised 15 December 2010; accepted 21 December 2010; published online 11 March 2011

Human CD52 is a glycosylphosphatidylinositol-anchored antigen expressed on the cell surfaces of normal and malignant lymphocytes.[9–11] Although the function of CD52 is largely unknown, CD52 is a favored target for lymphoma therapy and immunosuppression before bone marrow transplantation.[12–15] Alemtuzumab (CAMPATH-1H; Genzyme, Cambridge, MA, USA) is a recombinant humanized monoclonal antibody targeting the CD52 antigen.[16,17] The binding of CAMPATH-1H to CD52 on lymphocytes induces complement-dependent cytotoxicity (CDC),[18,19] antibody-dependent cell-mediated cytotoxicity (ADCC)[20–22] and direct cytotoxicity.[23,24] Here, we examined the cytotoxic effects of CAMPATH-1H on EVI1^{High} leukemia cells *in vitro* and the effects of CAMPATH-1H treatment on tumor growth in immunodeficient NOD/Shi-scid/IL-2Rγnull (NOG) mice xenografted with EVI1^{High} leukemia cells. Because CAMPATH-1H showed a direct cytotoxic effect, CDC and ADCC activity, as well as an *in vivo* antitumor effect against EVI1^{High} AML cells, CAMPATH-1H is likely to be a good therapeutic agent for AML with EVI1^{High} expression.

Materials and methods

Cell lines

UCSD/AML1 (refs 25, 26) cells derived from human AML were cultured in RPMI 1640 medium (Wako, Osaka, Japan) supplemented with 10% fetal bovine serum and 1 ng/ml granulocyte–macrophage colony-stimulating factor. Seven cell lines, U937 (ref. 27), K562 (ref. 28), KG-1 (ref. 29), HEL (ref. 30), HL60 (ref. 31), THP-1 (ref. 32) and HNT-34 (ref. 33), were purchased from the RIKEN Cell Bank (Tsukuba, Japan). MOLM1 (ref. 34) was purchased from the Hayashibara Institute (Okayama, Japan). Kasumi-3 (refs. 35, 36) was kindly provided by Dr Asoh (Hiroshima University, Hiroshima, Japan). K051 and K052 (ref. 37) were kindly provided by Dr Nomura (Nippon Medical School, Tokyo, Japan). NH was kindly provided by Dr Suzukawa (University of Tsukuba, Tsukuba, Japan). FKH-1 (ref. 38) and OIH-1 (ref. 39) were kindly provided by Dr Hamaguchi (Musashino Red Cross Hospital, Tokyo, Japan). U937, K562, HL60, THP-1, K051, K052, NH, HNT-34, MOLM1 and Kasumi-3 were cultured in RPMI 1640 medium (Wako) supplemented with 10% fetal bovine serum. The UCSD/AML1, MOLM-1, HNT-34 and Kasumi-3 cell lines each have chromosome 3q26 abnormalities with an EVI1^{High}, whereas U937, K562, KG-1, HEL, HL-60, THP-1, K051, K052, NH, FKH-1 and OIH-1 do not have 3q26 abnormalities and show a low EVI1 expression (Supplementary Table 1).

Patient samples

Leukemia cells were obtained from the peripheral blood (PB) of AML patients who had a blast population of more than 80% in

their PB at diagnosis before chemotherapy (Supplementary Table 2). After Ficoll–Hypaque (Sigma, Saint Louis, MO, USA) separation of the PB, the purity of the blast cells was confirmed by flow cytometry using immunofluorescence staining of phycoerythrin-conjugated CD11b and CD33 (Supplementary Figure S2). The study was approved by the Institutional Review Board of the Faculty of Medicine, University of Miyazaki. Informed consent was obtained from all blood and tissue donors according to the Declaration of Helsinki.

Antibodies

The human monoclonal antibody CAMPATH-1H that recognizes CD52 was obtained from Bayer Schering Pharma AG (Berlin-Wedding, Germany). The antibody against caspase-3 was commercially obtained from Cell Signaling Technologies (Beverly, MA, USA; catalog no. 9251).

Oligonucleotide microarray

The protocol used for the sample preparation and microarray processing is available from Affymetrix (Santa Clara, CA, USA). Briefly, at least 5 μg of purified RNA was reverse transcribed using Superscript II reverse transcriptase (Life Technologies, Grand Island, NY, USA) with the primer T7-dT24 containing a T7 RNA polymerase promoter. After a second strand of cDNA was synthesized with RNase H, *Escherichia coli* DNA polymerase and *E. coli* DNA ligase, the cDNA was transcribed *in vitro* to produce biotin-labeled cRNA with a MEGAscript High Yield Transcription Kit (Ambion, Austin, TX, USA) as recommended by the manufacturer. After the cRNA was linearly amplified with T7 polymerase, the biotinylated cRNA was cleaned with an RNeasy Mini Column Kit (Qiagen, Valencia, CA, USA), fragmented to 50–200 nucleotides, and then hybridized to the Affymetrix Human Genome U133 Plus 2.0 Array. The stained microarray was scanned with a GeneArray Scanner (Affymetrix) and the intensity of the signal was calculated with Affymetrix software, Microarray Suite 5.0. All data were scaled with the global scaling method to adjust the target intensity to 300. Then, we chose those genes with at least a 10-fold increase in the expression of the EVI1^{High} AML cells compared with low levels of EVI1 (EVI1^{Low}) AML cells with a statistical significance of P less than 0.01 by the t-test.

Reverse-transcription polymerase chain reaction

The levels of CD52, EVI1 and β-actin mRNA in the AML cells were measured by RT-PCR. Briefly, total RNA was extracted using Trizol (Invitrogen, Carlsbad, CA, USA), and 1 mg of total RNA was reverse-transcribed to obtain first-strand cDNA using an RNA-PCR kit (Takara-Bio Inc., Tokyo, Japan). cDNA fragments were amplied by PCR using specic primers. The primers used were as follows: CD52 forward, 5′-CATCAGCCTC CTGGTTATGG-3′, reverse, 5′-AAATGCCTCCGCTTATGTTG-3′; EVI1 forward, 5′-CACATTCGCTCTCAGCATGT-3′, reverse, 5′-ATTTGGGTTCTGCAATCAGC-3′; and β-actin forward, 5′-G ACAGGATGCAGAAGGAGATTACT-3′, reverse, 5′-TGATCCA CATCTGCTGGAAGGT-3′.

Establishment of stable U937 cell lines expressing EVI1

pGCDMsam-EVI1-IRES-EGFP was kindly provided by Dr A Iwama (Chiba University, Chiba, Japan). To produce recombinant retrovirus, the plasmid DNA was transfected into 293gp cells along with the vesicular stomatitis virus G expression plasmid by $CaPO_4$ co-precipitation. For retroviral transduction, 1×10^5 U937 cells were plated in 96-well flat-bottomed plates and were infected with either an EVI1 retroviral supernatant (pGCDMsam-EVI1-IRES-EGFP) or a mock retroviral supernatant (pGCDMsam-IRES-EGFP) with 100 ng/ml polybrene for 24 h. After 7 days, green fluorescent protein-positive U937 cells were sorted with a JSAN cell sorter (Bay Bioscience, Kobe, Japan).

Establishment of stable UCSD/AML1 cell lines expressing shEVI1

A DNA-based small hairpin (sh) RNA expression vector (pSIREN-retroQ-ZsGreen plasmid; Takara-Bio, Inc.) was used in the EVI1 knockdown experiment. The following sequence was cloned into the *Bam*HI–*Eco*RI site of the plasmid to create an shRNA against human EVI1: (ref. 22) 5′-GATCGCTCTAAGG CTGAACTAGCAGTTCAAGAGACTGCTAGTTCAGCCTTAGATT TTTTG-3′. A pSIREN-retroQ-ZsGreen-shLuc plasmid containing shRNA against luciferase (Takara-Bio Inc.) was used as a control. Retroviral particles were generated using the p10A1 packaging vector (Takara-Bio Inc.) and transient transfection of the 293T cell line, which was carried out with a Hilymax liposome transfection reagent (Dojindo, Kumamoto, Japan). For retroviral infection, 1×10^6 UCSD/AML1 cells were placed in 6 cm dishes containing 5 ml of retroviral supernatant with 100 ng/ml polybrene for 24 h. ZsGreen-positive UCSD/AML1 cells were sorted with a JSAN cell sorter (Bay Bioscience) 2 weeks after viral infection. The repression of EVI1 expression was confirmed by RT-PCR as described above.

Flow cytometry analysis

The cells were stained with the biotinylated CAMPATH-1H on ice for 15 min. They were washed and then labeled with a phycoerythrin-labeled streptavidin antibody on ice for 15 min. After washing, the treated cells were analyzed on a FACScan (Becton Dickinson, San Jose, CA, USA).

Cell growth inhibition assay

Leukemia cells (2×10^5 cells per ml) were incubated with various concentrations of CAMPATH-1H in complete medium at 37 °C in 5% CO_2. The cell growth was evaluated with the Trypan blue exclusion assay. The live cells were enumerated after Trypan blue staining using light microscopy.

Apoptosis assay

Apoptosis assays were performed using the Apoptosis Detection kit (MBL, Nagoya, Japan) according to the manufacturer's protocol. UCSD/AML1, HNT-34 or PT8 cells (2×10^5 cells per ml) were incubated with CAMPATH-1H (10 μg/ml) in complete medium at 37 °C in 5% CO_2 for 48 h. The cells were washed and resuspended in binding buffer at a concentration of 1×10^6 cells per ml. The suspension was then incubated with 5 μl of Annexin-V and 5 μl of propidium iodide for 15 min at room temperature in the dark. Samples were analyzed using a FACScan (Becton Dickinson). Annexin-V-positive cells were considered apoptotic.

Cytotoxicity assays

The CDC and ADCC activities of CAMPATH-1H were measured by a lactate dehydrogenase (LDH)-releasing assay using a cytotoxicity detection kit (Roche, Indianapolis, IN, USA). EVI1^{High} AML cells (1×10^4) were incubated with various concentrations of CAMPATH-1H and human serum as the

source of complement at a dilution of 1:6 (for the CDC assay) or with human PB mononuclear cells as effector cells (effector: target, 50:1 for the ADCC assay) in supplemented RPMI 1640 at 37 °C in 96-well flat-bottomed plates. After an additional incubation for 4 h at 37 °C, the extent of cell lysis was determined by measuring the amount of LDH released into the culture supernatant. The maximum LDH release was determined for cells lysed with 2% Triton X-100. The percentage of specific lysis was calculated according to the following formula: CDC % specific lysis = $100 \times (E-S)/(M-S)$, where E is the absorbance of the experimental well, S is the absorbance in the absence of monoclonal antibody (cells were incubated with medium and complement alone) and M is the maximum release of target cells (activity released from target cells lysed with 2% Triton X-100); ADCC % specific lysis = $100 \times (E-S_E-S_T)/(M-S_E)$, where E is the experimental release (supernatant activity from target cells incubated with antibody and effector cells), S_E is the spontaneous release in the presence of effector cells with antibody (supernatant activity from target cells incubated with effector cells), S_T is the spontaneous release of target cells (supernatant activity from target cells incubated with medium alone) and M is the maximum release of target cells (activity released from target cells lysed with 2% Triton X-100).

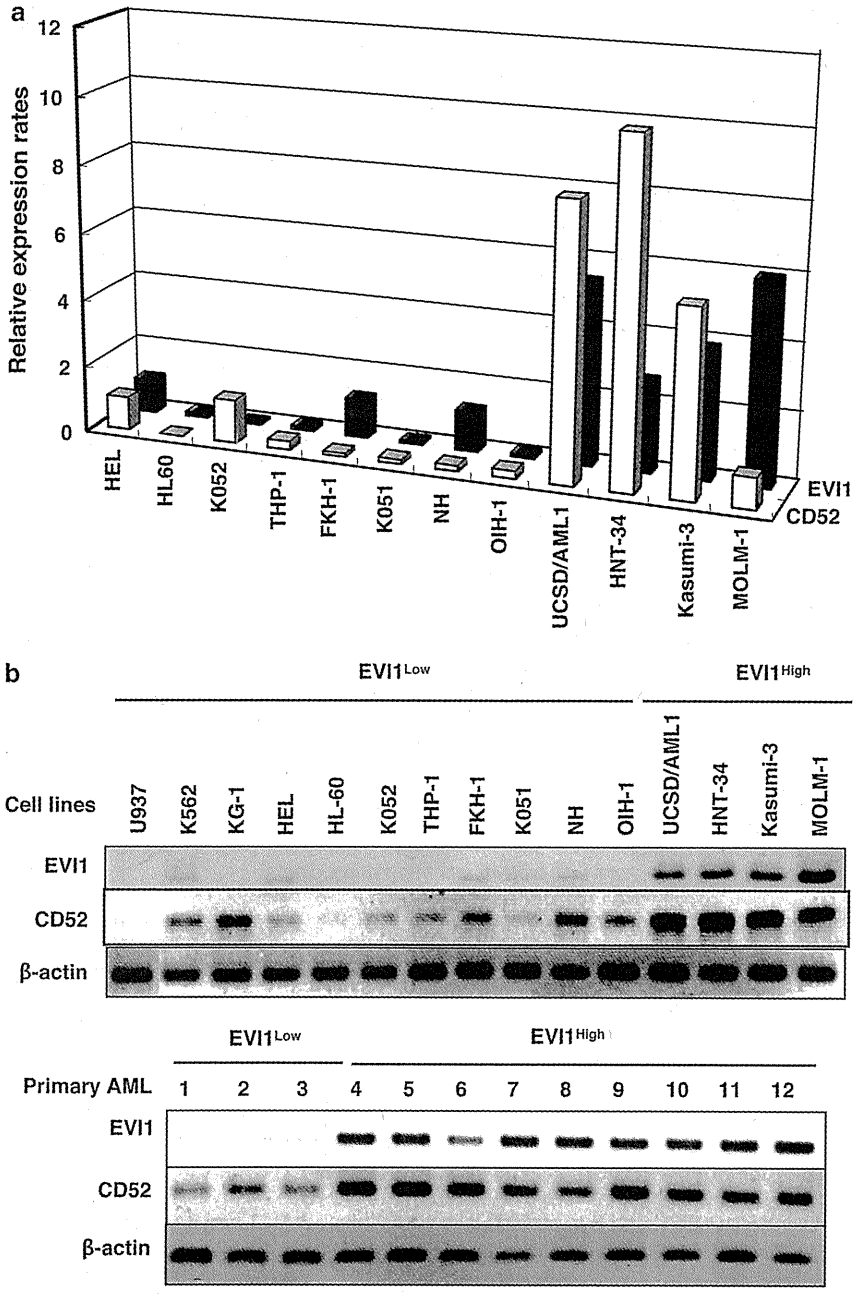

Figure 1 CD52 is highly expressed in EVI1^{High} myeloid leukemia cells. (**a**) The expression profiles of CD52 mRNA by DNA microarray. RNA samples from eight EVI1^{Low} and four EVI1^{High} AML cell lines were used for determining the gene expression profiles. (**b**) Semiquantitative RT-PCR analysis for EVI1 and CD52 is shown for 11 EVI1^{Low} and four EVI1^{High} AML cell lines (top panel), as well as primary AML cells from three patients with EVI1^{Low} and from nine patients with EVI1^{High} expression (bottom panel). The expression of β-actin is shown at the bottom as a control.

Xenograft tumors

Six- to eight-week-old female NOG mice were given a single subcutaneous injection of 5×10^6 UCSD/AML1 cells suspended in 100 µl phosphate-buffered saline (PBS) and mixed with an equal volume of Matrigel (BD Matrigel, BD Biosciences, Bedford, MA, USA). Xenografts were allowed to establish to an average size of 50–100 mm^3, after which mice were randomized into two groups. The groups of mice were given either PBS or CAMPATH-1H at a dose of 100 µg weekly intravenously for 4 weeks. Tumor volumes were derived as the product of the length, width and height of the tumor measured once a week with a caliper. A Kaplan–Meier survival analysis was performed using StatView (SAS Institute, Cary, NC, USA).

Data analysis

A faculty statistician analyzed the data. *P*-values were calculated using the Student's *t*-test for a comparison of independent data sets. Differences were considered statistically significant if the *P*-value was less than 0.05.

Results

EVI1^{High} myeloid leukemia cells express high levels of CD52

To search for novel molecular targets in refractory myeloid leukemia with EVI1^{High}, we initially analyzed the gene expression profiles of 12 human myeloid cell lines using an oligonucleotide microarray (Human Genome U133 Plus 2. 0 Array; Affymetrix) containing 38 500 genes. Four cell lines with chromosome 3q26 abnormalities (UCSD/AML1, HNT-34, Kasumi-3 and MOLM-1) expressed EVI1^{High}, and eight myeloid cell lines without chromosome 3q26 abnormalities (HEL, HL-60, K052, THP-1, FKH-1, K051, NH and OIH-1) expressed EVI1^{Low} (Figure 1a). When the expression profiles between EVI1^{High} and EVI1^{Low} leukemia cell lines were compared, we detected 26 genes that were upregulated over 10-fold in EVI1^{High} leukemia cells when compared with EVI1^{Low} leukemia cells ($P<0.01$) (Table 1). Among these genes, nine genes encode membrane proteins containing extracellular domains. These genes include the CD52 antigen (CAMPATH-1 antigen).

Table 1 Highly expressed genes in EVI1^{High} AML cells compared with EVI1^{Low} AML cells

Gene symbol	*Description*	*Fold change*	*Localization*
EVA1	*Epithelial V-like antigen 1*	54.98	Membrane/extracellular
MMRN1	*Multimerin 1*	49.34	Membrane/extracellular
LOC284262	*Hypothetical protein LOC284262*	47.46	Unknown
EHD2	*EH-domain containing 2*	44.45	Membrane/nucleus
SETBP1	*SET-binding protein 1*	40.48	Nucleus
CALCRL	*Calcitonin receptor-like*	38.95	Membrane/extracellular
CLEC7A	*C-type lectin domain family 7, member A*	32.33	Cytoplasm/membrane
PTPRM	*Protein tyrosine phosphatase, receptor type, M*	26.07	Membrane/extracellular
LCK	*Lymphocyte-specific protein tyrosine kinase*	24.61	Kinase/cytoplasm
ITGA6	*Integrin, alpha 6*	23.83	Membrane/extracellular
CD52	*CD52 antigen (CAMPATH-1 antigen)*	19.35	Membrane/extracellular
DEPDC2	*DEP domain containing 2*	18.45	Intracellular
PTRF	*Polymerase I and transcript release factor*	17.28	Intracellular
S100Z	*S100 calcium-binding protein, zeta*	16.21	Intracellular
RASGEF1B	*RasGEF domain family, member 1B*	14.88	Intracellular
GPR56	*G-protein-coupled receptor 56*	13.98	Membrane/extracellular
PHLDA2	*Pleckstrin homology-like domain, family A, member 2*	13.88	Intracellular
CD300A	*CD300A antigen*	13.08	Membrane/extracellular
TRPS1	*Trichorhinophalangeal syndrome I*	12.55	Nucleus
DPP4	*Dipeptidylpeptidase 4 (CD26, adenosine deaminase complexing protein 2)*	12.07	Membrane/cytoplasm
TNFSF8	*Tumor necrosis factor (ligand) superfamily, member 8*	11.89	Membrane/extracellular
FLJ11996	*Hypothetical protein FLJ11996*	11.48	Unknown
GNGT2	*Guanine nucleotide-binding protein (G protein), gamma-transducing activity polypeptide 2*	11.03	Membrane/cytoplasm
MFAP3L	*Microfibrillar-associated protein 3-like*	10.98	Membrane/extracellular
SYTL4	*Synaptotagmin-like 4 (granuphilin-a)*	10.27	Secretion

Abbreviations: AML, acute myeloid leukemia; EVI1, ecotropic viral integration site 1.
A list of genes that were selected by expression levels greater than 100 and an over 10-fold increased expression in EVI1^{High} AML cells than that in EVI1^{Low} AML cells with significant differences ($P<0.01$). Fold changes were calculated by the mean expression values of EVI1^{High} AML cells compared with EVI1^{Low} AML cells.

Figure 2 EVI1-dependent expression of CD52 in AML cells. (**a**) The expression of CD52 on various leukemic cells by flow cytometry using CAMPATH-1H. Cells were stained with phycoerythrin-labeled CAMPATH-1H, followed by analysis in an FACS. Figures show representative FACS histogram profiles of normal lymphocytes (PBL) and B lymphoid leukemia cell lines (BALL1 and RAMOS) in the upper panel, EVI1^{Low} AML cell lines (U937, NH and K562) in the second panel, EVI1^{High} AML cell lines (UCSD/AML1, HNT-34, Kasumi-3 and MOLM1) in the third panel and primary leukemic cells from patients with EVI1^{Low} (PT1) or EVI1^{High} (PT8, PT9 and PT11) AML in the bottom panel. Open histograms represent cells stained with isotype IgG controls and filled histograms indicate cells stained with CAMPATH-1H. (**b**, **c**) The induction of CD52 expression by a forced expression of EVI1 in U937 with EVI1^{Low} expression. Panel b shows the expression level of CD52 in parental, mock or EVI1 transfectant U937 cells by RT-PCR, and panel c shows the CD52 expression by FACS analysis. (**d**, **e**) The introduction of the shEVI1 expression vector in UCSD/AML1 cells with EVI1^{High} expression decreases CD52 expression. Panel d shows the CD52 mRNA level in parental, control shLuc or shEVI1 transfectant UCSD/AML1 cells by RT-PCR, and panel e shows the CD52 expression by FACS analysis.